SURFACE FREE ENERGY EVALUATION, PLASMA SURFACE MODIFICATION AND BIOCOMPATIBILITY STUDIES OF PMMA FILMS

A THESIS SUBMITTED TO
THE GRADUATE SCHOOL OF NATURAL AND APPLIED SCIENCES
OF
MIDDLE EAST TECHNICAL UNIVERSITY

BY

CANTÜRK ÖZCAN

IN PARTIAL FULFILLMENT OF THE REQUIREMENTS
FOR
THE DEGREE OF MASTER OF SCIENCE
IN
CHEMISTRY

JULY 2006

Approval of the Graduate School of Natural and Applied Sciences

Prof. Dr. Canan ÖZGEN
Director

I certify that this thesis satisfies all the requirements as a thesis for the degree of Master of Science.

Prof. Dr. Hüseyin İŞÇİ
Head of Department

This is to certify that we have read this thesis and that in our opinion it is fully adequate, in scope and quality, as a thesis and for the degree of Master of Science.

Prof. Dr. Nesrin HASIRCI
Supervisor

Examining Committee Members

Prof. Dr. İskender YILGÖR (KU, CHEM) _____

Prof. Dr. Nesrin HASIRCI (METU,CHEM) _____

Prof. Dr. Duygu KISAKÜREK (METU,CHEM) _____

Prof. Dr. Ali USANMAZ (METU,CHEM) _____

Prof. Dr. Erdal BAYRAMLI (METU,CHEM) _____

I hereby declare that all information in this document has been obtained and presented in accordance with academic rules and ethical conduct. I also declare that, as required by these rules and conduct, I have fully cited and referenced all material and results that are not original to this work.

Name, Last name: Cantürk, Özcan

Signature :

ABSTRACT

SURFACE FREE ENERGY EVALUATION, PLASMA SURFACE MODIFICATION AND BIOCOMPATIBILITY STUDIES OF PMMA

Özcan, Cantürk

M.S., Department of Chemistry

Supervisor: Prof. Dr. Nesrin HASIRCI

July 2006, 83 pages

PMMA is a widely used biomaterial especially in the fields of orthopedia, orthodontia and ophthalmology. When biocompatibility is considered, modification of the biomaterials' surface may be needed to optimize interactions of the biomaterial with the biological environment. After the surface modifications one of the most important changes that occur is the change in the surface free energy (SFE). SFE is an important but an obscure property of the material and evaluation methods with different assumptions exist in the literature. In this study, SFE of pristine and oxygen plasma modified PMMA films were calculated by means of numerous theoretical approaches (Zisman, Saito, Fowkes, Berthelot, Geometric and Harmonic Mean and Acid-Base) using numerous liquids and the results were compared to each other to elucidate the differences of methods. Dispersive, polar, acidic and basic components of the SFE were calculated by the use of different liquid couples and triplets with the application of Geometric and Harmonic mean methods and Acid-Base approach. The effect of SFE and the components of SFE on the cell attachment efficiencies were examined by using fibroblast cells. It was observed that with the treatment of oxygen plasma, cell attachment capability and hydrophilicity of PMMA surfaces were altered depending on the applied power and duration of the plasma.

Keywords: Surface free energy, acidic-basic components, dispersive and polar components, contact angle, geometric mean, harmonic mean, Zisman, Saito, Fowkes, Berthelot, PMMA, plasma surface modification, cell attachment, work of adhesion.

öz

PMMA FİLMLERDE YÜZEY ENERJİSİ HESAPLAMASI, PLAZMA İLE YÜZEY MODİFİKASYONU VE BİYOUYUMLULUK ÇALIŞMALARI

Özcan, Cantürk

Yüksek Lisans, Kimya Bölümü

Tez Yöneticisi: Prof. Dr. Nesrin HASIRCI

Temmuz 2006, 83 sayfa

PMMA özellikle ortopedi, ortodonti ve oftalmolojide yaygın olarak kullanılan bir biyomalzemedir. Biouyumluluk söz konusu olduğunda, biomateryalin biyolojik çevre ile yüzey etkileşimini optimize edebilmek amacıyla, yüzey modifikasyonu gerekebilir. Yüzey modifiye edildiğinde, yüzey enerjisi değişimi, oluşan en önemli değişimlerden biridir. Yüzey enerjisi bulunması zor olan ama önemli bir parametredir ve literatürde değişik yaklaşımlar ile yüzey enerjisi bulma metodları bulunmaktadır. Bu çalışmada hazırlanmış ve oksijen plazma ile modifiye edilmiş PMMA filmlerinin yüzey enerjileri farklı sıvılar ve birçok teorik yaklaşım kullanılarak (Zisman, Saito, Fowkes, Berthelot, Geometrik ve Harmonik Ortalama ve Asit-Baz) hesaplanmış ve metodlar arasındaki farklılıkları gözlemlemek amacıyla elde edilen sonuçlar karşılaştırılmıştır. Farklı olan ikili ve üçlü sıvı birleşimleri kullanılarak, Geometrik ve Harmonik ortalama ve Asit-Baz yaklaşım metodları uygulanarak yüzey enerjisinin polar, apolar, asidik ve bazik bileşenleri hesaplanmıştır. Yüzey enerjisi ve bileşenlerinin hücre yapışması üzerindeki etkisi fibroblast hücreler kullanılarak araştırılmıştır. Oksijen plazma uygulaması ile PMMA'ın hücre yapışması ve hidrofiliklik özelliğinin uygulanan plazma gücü ve süresi ile değiştiği gözlemlenmiştir.

Anahtar Kelimeler: Yüzey serbest enerjisi, asidik-bazik bileşenler, apolar ve polar bileşenler, temas açısı, geometrik ortalama, harmonik ortalama, Zisman, Saito, Fowkes, Berthelot, PMMA, plazma yüzey modifikasyonu, hücre yapışması, yapışma işi.

To My Dearest Grandmother, Mother and Father

ACKNOWLEDGEMENTS

I would like to express my great appreciation to Prof. Dr. Nesrin Hasırcı for accepting me to her lab group and guiding me through almost everything since my undergraduate years. She has always been a wonderful support and guidance in my life by any means.

Special thanks go to Tugba Endoğan and Esra Pınardağ for their very valuable friendship and moral support all through those hard times in my life. They both have always been there for me.

I am also thankful to Aysel Kızıltay, Eda Ayşe Aksoy and all the rest of my friends in our research group for their friendship and help.

I also would like to thank Özgür Kurç who helped me save time on creating computer programs for calculations.

Of all the souls in my life, I am exceptionally grateful to my dearest grandmother Ayşe Korürek, my mother Merih Özcan and my father Devrim Özcan for their unconditional love.

The last appreciation goes to the 'one' who will never be forgotten.

TABLE OF CONTENTS

LIST OF FIGURES

LIST OF TABLES

CHAPTER 1

INTRODUCTION

1.1 Surface

For a material, besides its bulk chemical and physical properties, surface is also one very important part since firstly it comes in contact and determines the compatibility with the environment. Thus, information about the properties of the surface means information about the behavior of the material towards other species. Parameters such as surface composition, surface topography and surface free energy (SFE) give information about the surface.

1.2 Surface Free Energy and Reactivity of Surfaces

Molecules at the surface are known to have different properties than the ones in the bulk. This arises from the fact that surface molecules experience different forces than the bulk molecules and these forces occur as a result of attractions between the neighboring molecules as well as the molecules that exist in the environment. The molecules in the bulk have no net force acting on them while the ones at the surface encounter a net force inwards as shown in Figure 1.1. This phenomenon results in a tension or free energy which is called 'Surface Tension' or 'Surface Free Energy' (SFE).

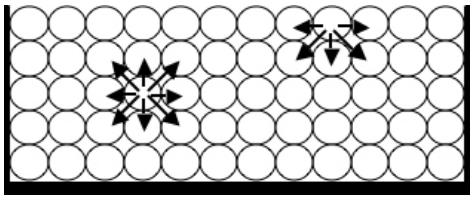

Figure 1.1 Liquid molecules and their interactive forces between them

SFE is defined as the work required to increase the area of a substance by unit amount and it has the units of mN/m or mJ/m^2 or dynes/cm [1].

Further information about the surface can be obtained from the components of it. SFE has polar (γ_s^p) and dispersive (γ_s^d) components which give information about the polar or apolar character of the surface. Their summation give the total SFE (γ_s^{Tot}) as shown in equation 1. In addition these polar constituents also have components (acidic and basic components mentioned in the following sections) which give more detailed information about the character of the surface.

$$\gamma_s^{Tot} = \gamma_s^d + \gamma_s^p \quad \text{..... 1}$$

SFE of a material allows one to predict the reactivity of the surface such as stain resistance, color stability and plaque resistance and therefore SFE is very important in many applications of biotechnology, biomedicine and industry [2].

1.3 Contact Angle

When a liquid is dropped on a solid substrate, a contact angle (θ) is formed which is defined as the angle between two of the interfaces at the three-phase line of contact as shown in Figure 1.2. These three phases are solid, liquid and gas (air usually). If water drops are used, contact angle values give information about the hydrophilicity and hydrophobicity of the solid surface. Contact angle of a liquid is the angle between the vectors A and B as shown in Figure 1.2 or simply the

angle of tangent to the circle of the liquid drop drawn from the point where the liquid drop touches the surface. In this figure vector A shows γ_{sl}, which is the interfacial tension between solid and liquid, vector B shows γ_{lv}, which is the interfacial tension between liquid and vapor and vector C shows γ_{sv}, which is the interfacial tension between solid and vapor.

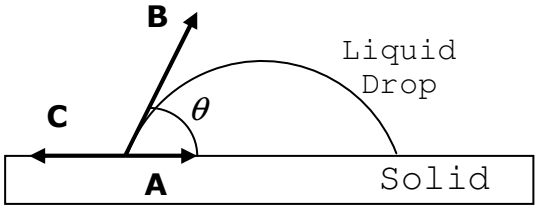

Figure 1.2 SFE vectors at equilibrium and contact angle.

Contact angle value of a liquid may range between 0 and 180 degrees. Zero contact angle means the surface is completely wetted by the liquid and the liquid and the surface are compatible to each other. Figure 1.3 shows two different liquid drops on the same polymer surface. The one that spread more (liquid B) has lower SFE than the other (liquid A) and has lower contact angle. Which means the attraction forces between the surface molecules and the liquid B molecules are higher than that of liquid A and the surface molecules. As a general trend the contact angle becomes lower when the SFE of the solid and liquid become closer.

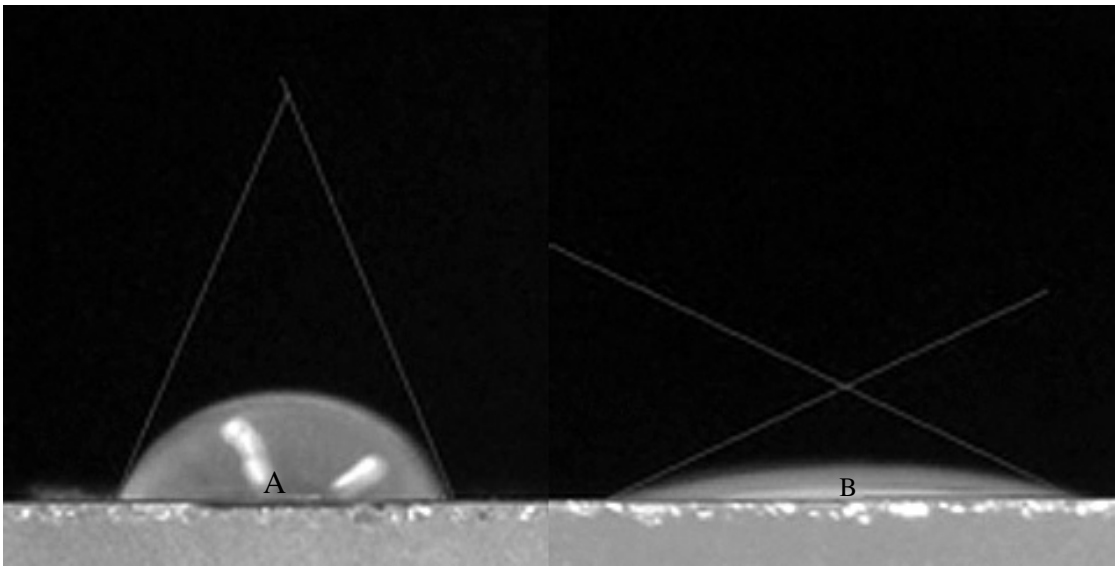

Figure 1.3 Two different liquid drops on a polymer surface.

When contact angle is to be measured, a given amount of liquid drop is usually deposited on the surface. If one continues to pump the liquid on the surface instead of placing a constant amount of liquid, the drop would start to grow on the surface and it would be exhibiting an advancing contact angle on the surface. And if that same drop is pulled back from the surface the liquid would be receding. Contact angle made by an advancing liquid (θ_a) and that made by a receding liquid (θ_r) may not be identical. This results in the so called contact angle hysteresis. Contact angle hysterisis is the difference between θ_a and θ_r. The reasons of contact angle hysteresis may arise from roughness and heterogeneity of the solid surface. Compared with chemically identical smooth surfaces, very rough surfaces give different contact angles which do not reflect material properties of the surface; rather, they reflect topographical properties [3].

1.3.1 Contact angle measurements

Contact angle measurements are usually carried out by goniometers which are based on taking a high quality photo of the liquid drop and measuring contact angle with the help of certain computer programs. This method is called drop shape analysis.

If the surfaces are rough or chemically heterogeneous, then contact angle measurements with drop deposition are meaningless; for an ideal surface on which no roughness and heterogeneity exist, there will be no contact angle hysteresis and the experimentally observed contact angle is equal to real θ.

1.4 SFE Measurements

SFE is an elusive quantity and there are several methods to obtain the SFE of a solid material by using contact angle values of various liquids. Different methods have singular assumptions and as a consequence, the results of them may have discrepancies.

The center of SFE estimation methods is the Young's equation which is given in equation 2. This equation interrelates the Young contact angle, θ, with the interfacial tensions of the liquid–vapor (γ_{lv}), solid–vapor (γ_{sv}), and solid–liquid (γ_{sl}) interfaces which are all in equlibrium [3].

$$\gamma_{sv} = \gamma_{sl} + \left(\gamma_{lv} Cos\,\theta\right) \quad \text{..... 2}$$

For low energy surfaces, γ_{sv} can be defined as γ_s, and γ_{lv} can be defined as γ_l [4].

1.4.1 Zisman Plot

Zisman's approach [4] was the earliest method to estimate the SFE. In this approach, the contact angles (θ) of multiple liquids with various SFE are obtained and $Cos\,\theta$ values are plotted against SFE of the liquids (Figure 1.4). To obtain the critical SFE of the solid, the Zisman Plot can be extrapolated to a value where $Cos\,\theta$ = 1, that is θ = 0 and the liquid completely spreads on the solid. The critical SFE is conceptually related to the SFE [1].

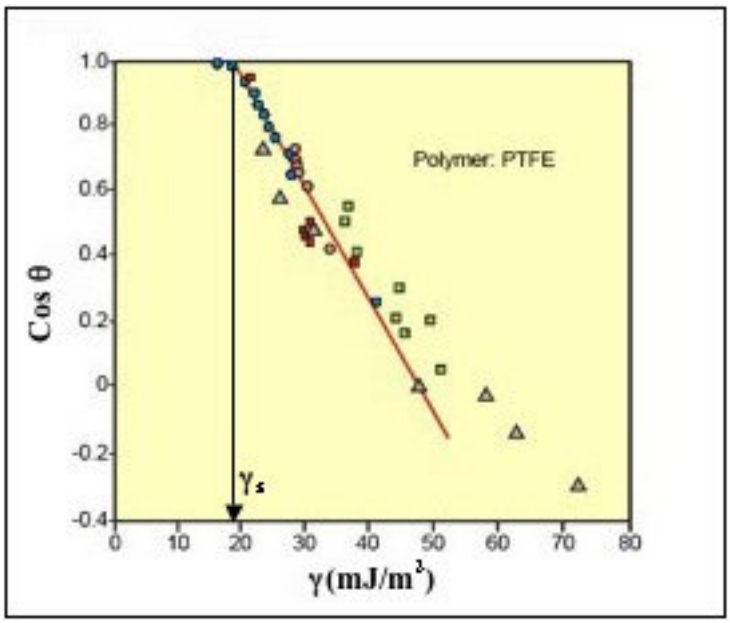

Figure 1.4 Zisman Plot [5]

The test liquids used in Zisman Plot should neither interact nor react with the surface. In addition they need to constitute a homologous series of liquids in order to discard geometrical effects. This may put a limitation to the Zisman Plot measurements. Another limitation of the Zisman plot is the impossibility of estimation of polar and dispersive components of SFE.

1.4.2 Saito Plot

Saito proposed another plot, which also makes it possible to find the SFE of a material. This plot is similar to Zisman plot, however, log $(1+Cos\,\theta)$ is plotted versus log (γ_l). The surface free energy of the solid surface is determined from the point where θ is zero as in the Zisman plot, however, SFE is found from the point which corresponds to a y axis value which is equal to log 2. The advantage of this plot is that homologous series of liquids are not required as they do in Zisman plot.

1.4.3 Work of Adhesion

The work required to separate a unit area of interface between two phases is called work of adhesion. Work of adhesion, W_{sl}, for a solid-liquid interface is generally defined as;

$$W_{sl} = \gamma_l + \gamma_s - \gamma_{sl} \quad \text{..... 3}$$

Combination of equation 2 and 3 redefines the work of adhesion as;

$$W_{sl} = \gamma_l (1 + Cos\ \theta) \quad \text{..... 4}$$

With equation 4, one can simply find the work of adhesion by measuring the contact angle of a liquid since the liquid surface free energy, γ_l, is known.

The adhesion of a substance or a cell to a surface involves a finite amount of energy which is also referred to as work of adhesion. Its extent decides the scope of adhesion of a material on a certain surface. So possibility of adhesion process on a given surface can be predicted by the magnitude of work of adhesion which makes it a very useful parameter for characterizing biomaterials [6].

Different assumptions for work of adhesion exist in literature which are discussed in the proceeding sections. These lead to other valuable equations that makes it possible to find SFE in different ways which are shown in the subsequent sections.

1.4.4 Berthelot's Approach

Berthelot approximated the work of adhesion for a solid-liquid interface by a geometric mean as in equation 5 which made it possible to estimate SFE with a different equation.

$$W_{sl} = 2\sqrt{\gamma_l \gamma_s} \quad \text{..... 5}$$

Combination of equation 4 and 5 yields;

$$Cos\ \theta = -1 + 2\sqrt{\frac{\gamma_s}{\gamma_l}} \quad \text{..... 6}$$

This equation is a very simple tool to estimate the SFE since it requires only one liquid's data. However, use of single liquid's data may not be sufficient and this equation over-estimates the interaction between unlike molecules. In addition, this equation may generate largely deviating results with different liquids [4]. Girifalco and Good introduced a parameter (ϕ) into the equation 5 which takes into account the possible deviations of the equation. Different proposals for the parameter are available in the literature [4, 7, 8].

1.4.5 Geometric Mean and Harmonic Mean Approaches

Surface free energy may also be obtained from the Geometric and Harmonic mean methods by the help of contact angles of liquids on the solid surface.

Geometric and Harmonic mean equations not only give the SFE but they also allow the estimation of polar and dispersive components of SFE. As mentioned previously SFE may be written as in equation 1, where the superscript 'd' denotes the dispersive (or Lifshitz–van der Waals) component and 'p' denotes the polar component. Combination of Young's equation (equation 2) with Harmonic (equation 7) or Geometric (equation 8) Mean equations lead to other equations that are helpful to find the components of SFE.

Harmonic Mean Equation:

$$\gamma_{sl} = \gamma_s + \gamma_{lv} - 4\left(\frac{\gamma_{lv}^d \gamma_s^d}{\gamma_{lv}^d + \gamma_s^d} + \frac{\gamma_{lv}^p \gamma_s^p}{\gamma_{lv}^p + \gamma_s^p} \right) \quad \text{..... 7}$$

Geometric Mean Equation:

$$\gamma_{sl} = \gamma_s + \gamma_{lv} - 2\left(\left(\gamma_{lv}^d \gamma_s^d \right)^{1/2} + \left(\gamma_{lv}^p \gamma_s^p \right)^{1/2} \right) \text{..... 8}$$

Combination of equation 2 and 7 leads to:

$$\gamma_{lv}(1 + Cos\,\theta) = 4\left(\frac{\gamma_{lv}^d \gamma_s^d}{\gamma_{lv}^d + \gamma_s^d} + \frac{\gamma_{lv}^p \gamma_s^p}{\gamma_{lv}^p + \gamma_s^p} \right) \quad \text{..... 9}$$

Combination of equation 2 and 8 leads to:

$$\gamma_{lv}(1 + Cos\,\theta) = 2\left(\left(\gamma_{lv}^d \gamma_s^d \right)^{1/2} + \left(\gamma_{lv}^p \gamma_s^p \right)^{1/2} \right) \text{..... 10}$$

The use of equations 9 and 10 would require dispersive and polar component values of two test liquids' surface tension data whose contact angles on the surface are known or obtained. Solving the equations for the surfaces by simultaneously putting the dispersive and polar component values of liquids' SFE lead to surface's energy components. This would necessitate the use of liquid pairs. However if one wants to use all the test liquids used in the experiment, equation 10 can be rewritten in the following form.

$$\frac{(1+Cos\,\theta)\gamma_{lv}}{2\sqrt{\gamma_{lv}^{d}}} = \sqrt{\gamma_{s}^{d}} + \sqrt{\gamma_{s}^{p}}\left(\frac{\sqrt{\gamma_{lv}^{p}}}{\sqrt{\gamma_{lv}^{d}}}\right) \quad \text{..... 11}$$

In this equation; if y and x are defined as:

$$y = \frac{(1+Cos\,\theta)\gamma_{lv}}{2\sqrt{\gamma_{lv}^{d}}} \quad \text{..... 12}$$

$$x = \frac{\sqrt{\gamma_{lv}^{p}}}{\sqrt{\gamma_{lv}^{d}}} \quad \text{..... 13}$$

Accordingly, a plot of y versus x would give the dispersive and polar components of the solid SFE by calculating the squares of the intercept and slope of the line.

When low water wettability is considered and since water is a higly polar molecule, it is reasonable to think that dispersive component dominates the surface free energy [9].

1.4.6 Fowkes Approach

It is also possible to find SFE from one liquid's data by Fowkes approach [4,8] as in the case of Berthelot's. However, this time dispersive component of the solid SFE is obtained. Assuming that only dispersive forces act across an interface Fowkes proposed that;

$$W_{sl} = \sqrt{\gamma_{l}^{d}\gamma_{s}^{d}} \quad \text{..... 14}$$

When the equations 4 and 14 are combined, it yields;

$$Cos\ \theta = -1 + 2\sqrt{\gamma_s^d}\ \frac{\sqrt{\gamma_l^d}}{\gamma_l} \quad \text{..... 15}$$

When a liquid's contact angle on the surface is known, the dispersive component can be found by using equation 15. One can also make use of all the test liquids when applying Fowkes method. A plot of $Cos\,\theta$ versus $\left[\frac{\sqrt{\gamma_l^d}}{\gamma_l}\right]$ would give the dispersive component from the slope.

A high value of dispersive component than that of polar component would mean the surface has non-polar character mainly. This non-polar character would be observed more for hydrocarbons, which generally have van der Waals forces as attractive forces between molecules and have commonly no polar component of SFE. On the other hand, a high value of polar component compared to dispersive component of SFE would mean the surface has more of a polar character.

1.4.7 Acid Base Approach

Besides the dispersive and polar components, SFE also has acidic and basic components. The acid base approach was proposed by van Oss, Good and Chaudhury [4]. Their perception was such that at the solid-liquid interface molecules can interact through electron donor/acceptor manner. Consequently according to acid-base approach, SFE is divided into Lifshitz-van der Waals component $\left(\gamma^{LW}\right)$ corresponding to dispersive attractions and acid-base component $\left(\gamma^{AB}\right)$ corresponding to polar attractions. This acid-base component is composed of acidic $\left(\gamma^{+}\right)$ and basic $\left(\gamma^{-}\right)$ components. Acidic component is the electron acceptor parameter and basic component is the electron donor parameter. If the acid-base component is zero then both the acidic and basic components

are also zero and the surface is said to be non-polar. If only one of the acidic and basic components have a value then the surface is considered monopolar and if the two have significant values then bipolar.

In the acid-base approach the work of adhesion is claimed as;

$$W_{sl} = 2\left(\sqrt{\gamma_l^{LW}\gamma_s^{LW}} + \sqrt{\gamma_l^{+}\gamma_s^{-}} + \sqrt{\gamma_s^{+}\gamma_l^{-}}\right) \quad \text{16}$$

Which leads to;

$$(Cos\,\theta + 1)\gamma_l = 2\left(\sqrt{\gamma_l^{LW}\gamma_s^{LW}} + \sqrt{\gamma_l^{+}\gamma_s^{-}} + \sqrt{\gamma_s^{+}\gamma_l^{-}}\right) \quad \text{17}$$

To solve equation 17, data obtained from at least three liquids is necessary. The choice of liquid triplet is a delicate one. It is also advised in the literature, to use at least one totally dispersive liquid [4].

It should be noticed that the acidic component of solid surface energy interacts with basic component of the liquid surface energy and vice versa.

1.5 Importance of SFE of Biomaterials

Knowledge of the reactivity or energy of surfaces, and in particular their interaction with fluids, is very important in the application of materials. As an example of such reactivity relation, the requirement of good wetting of tooth surfaces to achieve adhesion and the ability of materials in the mouth to avoid adhesion of salivary pellicle and bacterial plaque are two main areas of concern in the field of contemporary dentistry [1].

For attaching fixed prostheses and for bonding orthodontic appliances, adhesion is necessary. Sealants that prevent tooth decay are examples of this type of material. In addition, for the maintenance of removable prostheses, good wetting of denture surfaces is important. On the contrary, poor wetting of tooth substance and restorative materials by saliva is sometimes an advantage. Hydrophobic materials have better color stability and stain resistance. It can also be hypothesized that restorative materials with low surface energy resist plaque formation better than the ones with higher SFE. Furthermore for teeth and restorative materials it is necessary to develop plaque resistant coatings [1].

Many other biomaterials, used in distinctive medical fields, have varying hydrophilicities and SFE. However these differences in surface properties and their relation to biocompatibility is a very critical issue that needs to be addressed and completely understood by the science community. Advances achieved in this field, will make it possible to predict the biocompatibility of a material by simply measuring its SFE, rather than learning the biocompatibility of it from analysis of extensive biocompatibility tests.

1.6 Modification of the Surfaces of Polymeric Materials

Polymeric materials have a wide variety of applications in medical areas because of their desired mechanical strength, chemical stability, light weight, as well as their tailor made design possibilities. The most important point is inertness and biocompatibility of the material and polymers have great options on this aspect. However, in contact with biological systems, these materials are not always compatible. So modifications are necessary at the surfaces to perform the requirements of the desired medical applications [10].

Most synthetic biomaterials often result in a number of adverse physiological reactions such as thrombosis formation, inflammation and infection even though they have the physical properties that meet or

even exceed those of natural tissue. Modifying the surface of a material can improve its biocompatibility without changing its bulk properties [11].

To alter the interactions of polymers with their biological environments, modifications of their surface can be achieved by means of numerous processes such as plasma–ion beam treatment, electric discharge, surface grafting, chemical reaction, vapor deposition of metals and flame treatment (Table 1.1).

Table 1.1 Surface Modification Methods

Physical	**Chemical**	**Radiation**
Physical adsorption	Oxidation by strong acids	Plasma (glow discharge)
Langmuir-Blodgett film	Ozone treatment	Corona discharge
	Chemisorption	Photo activation (UV)
	Flame treatment	Laser
		Ion beam
		Electron beam
		Gamma irradiation

Changes in chemical group functionality, surface charge, hydrophilicity, hydrophobicity and wettability can be achieved surface modifications [12].

Interaction forces that emerge between a biomaterial's surface and a living system are due to the polymeric material's chemical and physical characteristics which are located within few Angstron to nanometers of the surface region [13]. Even, modification at a monomolecular level is enough to alter the wetting and adhesion properties of a material because the responsible intermolecular forces for wetting and adhesion are short ranged forces [14]. In this sense plasma application is a good technique for modification of the surfaces in a few molecular layers or in nano levels without altering the bulk properties.

1.6.1 Modification of PMMA Surface

PMMA surface chiefly consists of methyl ester groups which confines the standard chemical modification ways to two basic categories as photochemical and photophysical methods. Laser alteration or UV irradiation in air and "wet" chemical modifications are such examples. In wet chemical method mainly reduction of ester groups to alcohol occurs. Alternatively, amino functionalities may be formed on the surface through aminolysis of the ester groups. One other important modification is plasma treatment on PMMA. Many different types of gas-plasmas have been used including air, oxygen, UV-ozone, H_2O, ammonia and argon for modification. Because of chemical reactions and physical sputtering with active gas-phase species, plasma modification alters the chemical groups on the surface of PMMA [15].

1.6.2 Plasma Treatment for Modification of Surfaces

Plasma, which contains a wide variety of active particles and vacuum ultraviolet radiation is described as the fourth state of matter [2]. Different types of plasmas such as microwave, radio frequency, corona discharge, etc. are used to treat solid surfaces. This treatment is often used for modification of wettability, printability, adhesion, durability, hardness, membrane permeability and compatibility with living tissues. These plasma surface modifications exhibit complex, multifunctional chemistries, crosslinked and branched structures and changes in the carbon/hydrogen ratio. Many different types of reactions (such as oxidation, degradation, cross-linking, structural changes) may occur in the thin surface layer due to interaction of plasma with the solid material. Surface of the material changes its chemical and physical properties. Type of gas used, gas pressure, temperature, kind of solid surface, power and time of plasma action are the factors affecting the efficiency of these processes [2].

Plasma exist in the forms of high temperature and low temperature plasmas. High temperature plasma occurs at atmospheric pressure in either its manmade form such as a plasma torch or its natural form

such as lightning. Low temperature (also called low pressure) plasma techniques are suitable for modifying solid surfaces and improving their surface properties. In general, surface reactions, plasma polymerisation, cleaning and etching are classified as reactions of low pressure plasmas with solids. Uniformity and reproducibility, diversity of reagent gases and selective modification with minimal change in bulk property are advantages of low pressure plasma treatment as a surface modification technique over other techniques [2].

Electrons, ions, radicals and metastable species are involved in the process of plasma treatment. These species interact with the exposed surfaces causing some chemical changes at the surface of the material. If the applied energies are higher than the characteristic bonding energies of the polymers, some parts of the surface can undergo scission reactions and form new bonding configurations. Accordingly generation of new functionalities takes place as elementary processes in every plasma. Depending on the power applied and duration of application, either etching or coating dominates [10]. A schematic diagram of the plasma application in the reactor is given in Figure 1.5.

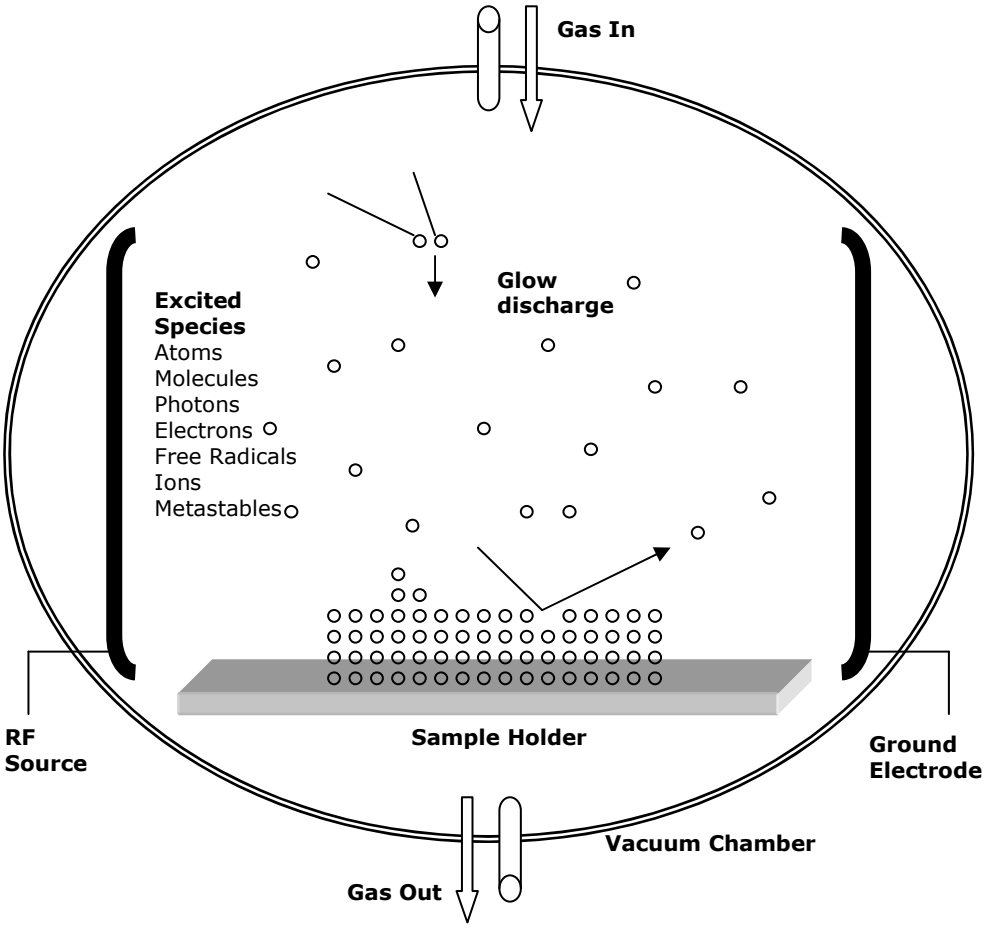

Figure 1.5 Plasma surface modification within the plasma reactor.

The detailed process of glow discharge plasma includes evacuation of an inert vessel and then refilling it with a low-pressure gas. Techniques such as, radiofrequency energy, microwaves and alternating current or direct current, energise the gas. As a result the energetic species like ions, electrons, radicals, metastables and photons in the short-wave ultraviolet (UV) range are formed. Surfaces in contact with gas plasmas are bombarded by these energetic species and their energy is transferred from the plasma to the solid. Surface modification is resulted from these energy transfers which are dissipated within the solid by a variety of chemical and physical processes [11]. These process are presented in Figure 1.6.

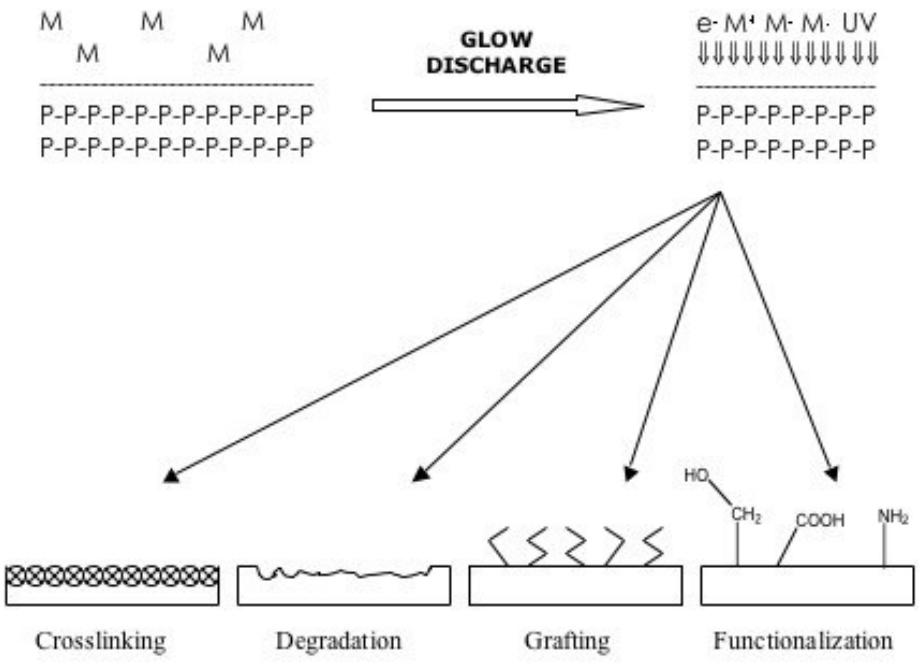

Figure 1.6 Reactions taking place in plasma surface modification.

Gas types, treatment power, treatment time and operating pressure, can be varied by the user as process parameters. System parameters such as electrode location, reactor design, gas inlets and vacuum are set by the design of the plasma equipment. Compared to the most other high-energy radiation processes, plasma process offers greater control due to these wide range of parameters [11].

The process can also be used to tailor surface energies. Plasma treatment generally increases the SFE of the material [16]. Hydrophilic and hydrophobic surfaces can be created on polymers through interaction with a gas plasma. If oxygen is used, oxygen functionality is created and this increases the wettability of the surface. This type of application has been used to enhance the performance of a catheter by the creation of a wettable surface on the polymer tubing. In a similar way, surfaces can be specifically modified for protein binding and improve blood compatibility [11].

Plasma modification is a preferable technique since it is effective at near-ambient temperature without damage to most heat-sensitive biomaterials. Modification of almost any kind of substrate geometry is possible with plasmas. Plasma also have the ability to functionalize surface, which chemical processing cannot offer. Other advantages include flexibility, effectiveness, safety and environmental friendliness [11].

Besides surface modifications, disinfection and sterilization of medical devices are other possible uses of plasma technology. The potential for simultaneous surface modification and sterilization in biomedical device fabrication is the most convenient aspect of plasma technology [11]. For example in the case of cell attachment tests, the modification and sterilization can be achieved at once.

1.7 Biocompatibility

1.7.1 Biocompatibility and Cell Adhesion

Biocompatibility is a desired characteristic of the materials used for the applications in the medical and pharmaceutical fields. The definition of biocompatibility by the European Society for Biomaterials is ‘‘the ability of a biomaterial to induce the appropriate answer in a specific application’’. For instance, for an implant, biocompatibility would mean being well accepted by the cells around it and proliferation of cells on the material. On the other hand, for a catheter situation would be the reverse. A catheter needs to prohibit cell growth in order to be compatible. As another example, for materials in contact with blood, compatibility means no coagulation of red blood cells [10]. Biomaterials that come in contact with blood or protein require special surface properties to enhance biocompatibility [11].

The most indicative processes to assess the biocompatibility of a synthetic surface is the cell adhesion and spreading [17]. Cells are regarded as deformable spheres, wrapped by polysaccharide coated membranes [18], which are the main parts of the cells that are

responsible for adhesion. The substrate and a cell or a particle in a liquid, exhibit short-range electrostatic repulsion and relatively longer-range attractive forces which need to be in balance for achieving adhesion. What drives cells to the surfaces like glass, polymers, metals, lipids and collagen is actually the attractive van der Waal's forces and plurivalent cation bridging [6].

Cell adhesion is triggered by protein adsorption which occurs immediately when an implant is placed into the body. It is believed that the first layer of protein adsorbed on the surface controls the cell attachment. Adsorption of adhesion promoting molecules such as fibronectin, collagen or laminin, which contain the tripeptide cell binding domain arginine-glycine-aspartic acid, promote cell adhesion. Another method is to create functional or reactive groups such as hydroxyl, carboxyl and amine on the surface to promote cell adhesion [13].

In addition to being capable of adhering cells, surfaces should have minimum foreign-body reactions. Surface functionalizations may be achieved by plasma treatment, which gives the opportunity of a vast range of chemical and physical modification possibilities only at the surface [13]. To enable covalent immobilization of cell-binding peptides derived from the extra cellular matrix proteins: fibronectin and laminin, surface activation of synthetic polymeric implant materials can be done by using radio frequency plasma techniques. The resulting grafted peptides can promote complete coverage of a surface with a monolayer of intact, healthy endothelial cells. This results in a natural blood compatible surface. An example is the ammonia plasma treatment, where amine functional groups form on the surface and they act as hooks for anticoagulants, such as heparin. As a result, reduction in thrombogenicity is achieved [11].

1.7.2 Biocompatibility and Use of Acrylic and Methacrylic Polymers as Biomaterials

Long-term biocompatibility and functionality of acrylic and methacrylic polymers, which are increasingly used as biomaterials for numerous

medical applications such as vascular grafts, drug releasing systems and intraocular or contact lenses, are strongly controlled by their in vivo interactions with the living tissues [19].

Poly (methyl methacrylate), PMMA, among other methacrylic polymers, has been extensively studied for the numerous applications in the field of coatings, adhesives, sensors, biomaterials and medical applications. PMMA has the privilege of being the first implanted biomedical polymer which has been used since the 1950's [20]. Understanding the surface properties of PMMA is very important when all of its biomedical applications are considered in terms of biocompatibility.

PMMA is widely engaged in ophthalmic, orthopaedic and dental applications in its different forms [21]. In dentistry, self-curing PMMA cements have been widely used. They are utilized in powder and liquid forms that are mixed at room temperature. They, then, self-polymerize. The powdered part mainly contains PMMA and the liquid part contains the monomer [22]. In the field of orthopedy, PMMA, among other bone cements, has been successfully used in surgeries. First use of PMMA as a bone cement goes back to 1960s. Even though this type of PMMA application has many advantages, its common use is restricted by several obstacles such as low adherence to bone surfaces and having monomer toxicity. In joint replacements, dissatisfaction took place mostly due to aseptic loosening and tissue necrosis even though replacements have been approximately 90% successful over the last 10 years [23].

Orthopedic and dental implants can be made more bone compatible by prevention of bacterial infection and by maintenance of osteoblast (bone cells) functions. This can be achieved by functionalized PMMA-based co- and ter-polymers [24]. Mixing PMMA and silica also improved attachment, proliferation and differentiation of osteoblast cells, in vitro, compared to pure PMMA. [25].

Utilization of PMMA in ophthalmology as an intraocular lens (IOL) has extensively taken place. The advantages of PMMA as IOL are its

outstanding optical and mechanical properties [15]. However in ophthalmology, cell adhesion to the biomaterial's surface may be a foreign body reaction and PMMA is not as biologically inert as considered [26]. On the other hand, weakening of the implant-host interface due to weak cell adhesion leads to separation and therefore loss of globe integrity [27]. So surface modifications should be made in such a way to boost attachment at the interface but lessen attachment when it comes down to interior parts. Increase in biocompatibility of IOL has been achieved by several ways such as, surface modification with heparin [26], by grafting di-amino-PEG (poly ethylene glycol) onto PMMA [27] and by ion implantation [15].

In addition, syntheses of linear polymers which possess sulfonate and carboxylate ionic groups were done to achieve functionalized PMMA based polymers for improved biocompatibility. In order to grant a random distribution of the ionic groups, polymers were synthesized by radical copolymerization of the appropriate monomers. Compared to the nonfunctionalized PMMA, these PMMA-based polymers largely prevent the proliferation of lens epithelial cells and fibroblasts without any additional cytotoxicity. Chemical composition of the PMMA-based polymer and the distribution of the anionic carboxylate and sulfonate groups are the constraints that are responsible for the biological inhibition. [28]

1.7.3 Biocompatibility-Surface Property Relation

It is crucial to obtain information about the surface properties of synthetic biomaterials in order to prevent harmful consequences. Surface properties of synthetic materials such as hydrophilic/hydrophobic balance, surface charge and SFE are dominant parameters for protein adsorption and cell attachment processes. In the sense of hydrophilicity, a moderately wettable surface is a quite good support for cell adhesion and proliferation, while superhydrophilic or superhydrophobic surfaces do not promote bioadhesion. On the other hand, strong negative surface charge on the material provides

long-range electrostatic repulsion since the living cells are negatively charged and rapid cell adhesion is prevented [19]. As a foreground to the cell adhesion, protein adsorption depends on chemical composition, surface structure and surface tension of the biomaterial. Introduction of amine or carboxylic functions causes bonding of proteins or protein segments and leading cells do not perceive the surface as a foreign material. In general protein adsorption is lowest if hydrophilic and less polar groups are available [10].

In addition to type of knowledge mentioned above, SFE and biocompatibility relation is a very important one that needs to be well understood to be able to deduce biocompatibility of the surfaces of biomaterials.

1.8 Aim of the Study

The correct way for the evaluation of SFE or the measurement of contact angle is still an unsolved discussion in the science community [29, 30]. Therefore, this study firstly aims to compare the well known methods for finding SFE and its components, for the pristine and oxygen plasma modified PMMA films.

In the second part of the study, the aim is to modify the surfaces of PMMA films at molecular level with the application of oxygen plasma and then examine the relation between the power applied and surface free energy as well as the components of surface free energy. This will be useful in selecting the modification conditions for various uses of PMMA.

In the last part of the study, the aim is to correlate the altered surface properties of the modified PMMA with biocompatibility by cell attachment experiments.

CHAPTER 2

MATERIALS AND METHODS

2.1 Materials

2.1.1 PMMA Substrate and Solvent

Poly (methyl methacrylate) (PMMA), $[-CH_2C(CH_3)(CO_2CH_3)-]_n$, with a molecular weight of 120 000, was purchased from Aldrich, Germany and used to prepare films. Chloroform, ($CHCl_3$) was purchased from Lab-Scan, Ireland and used as a solvent for PMMA.

2.1.2 Test Liquids

Tricresyl phosphate ($(CH_3C_6H_4O)_3PO$) and bromo napthalene ($C_{10}H_7Br$), were products of Aldrich (Germany), aniline ($C_6H_5NH_2$) and formamide ($HCONH_2$) were products of Merck (Germany). Diodomethane (CH_2I_2), glycerol ($CH_2OHCHOHCH_2OH$), ethlyene glycol ($HOCH_2CH_2OH$) and dimethyl sulfoxide (C_2H_6OS), were products of Acros (USA) and diethylene glycol ($O(CH_2CH_2OH)_2$) was a product of Fischer (USA). In all the experiments de-ionized triple distilled water was used. All of the liquids were reagent grade and used in contact angle measurements.

2.1.3 Materials Used in Cell Attachment Tests

Fetal bovine serum (FBS) was obtained from Biochrome KG (Germany). Dulbecco's Modified Eagle Medium (DMEM) was obtained from Gibco Invitrogen Corporation (New Zealand). MTS kit was purchased from Promega Corporation (USA). Cacodylic acid (sodium salt), glutharaldehyde (Grade I, 25 % aqueous solution), trypsin-EDTA (0.25 %), were supplied by Sigma Chemical Corporation (USA). Acridine Orange was obtained from BDH Chemicals Ltd. (UK). 3T3 cell line was purchased from Foot-and-Mouth Disease Institute of Ministry of Agriculture & Rural Affairs (Turkey).

2.2 Preparation of PMMA Films

PMMA films were prepared by solvent casting method. Solutions containing 20 % (w/w) PMMA in chloroform were prepared at room temperature and poured on microscope slides and let to dry. Solvent evaporation was achieved in an oven at room temperature for 5 to 7 days and then placed in vacuum oven at room temperature to remove the residual solvent. It was shown that solvent casting method gives minimum roughness to the surface [3]. For cell attachment tests, films were formed on Teflon sheets, dried as described, separated and cut into 1 cm^2 pieces by scissor.

2.3 Plasma Modification

Surface modification of polymers was achieved by Advanced Plasma Systems Inc. plasma system (USA) by placing microscope slides covered with PMMA films. The instrument used in this study is given in Figure 2.1. Instrument consists of vacuum chamber, manifold unit, vacuum pump, power distribution box, RF power supply and matching network.

Actual plasma process takes place in the vacuum chamber which consists of an aluminum container. It bears electrodes, purge inlet board, vacuum break and chamber door. Electrodes which are located inside the chamber are paired aluminum assemblies. During the plasma cycle, these assemblies are excited by RF generator, creating the actual plasma used for the treatment of the products. Manifold contains all the inlet and exhaust equipment to vent gases to and from the chamber. Vacuum pump unit consists of a two-stage mechanical pump that removes gases from the chamber, insuring a continuous flow. Matching network is used for matching the impedance of the RF source to the impedance of the chamber, eliminating reflected power. For RF power supply, Seren R300 13.56 MHz power generator is used.

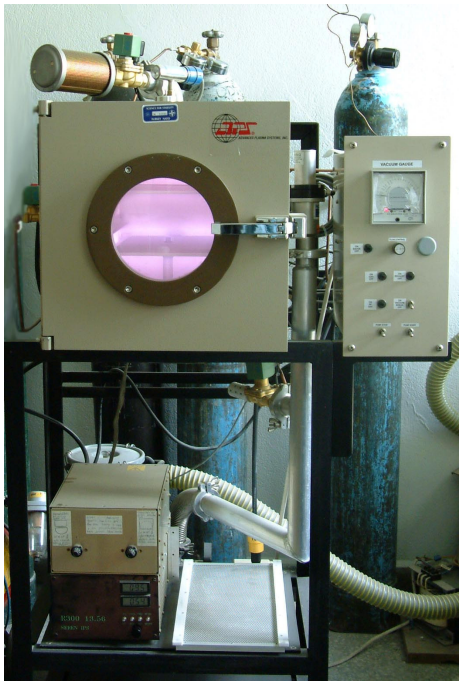

Figure 2.1 Plasma instrument

PMMA films were subjected to oxygen plasma treatment at different discharge powers (20, 100 and 300 Watts) and at two different treatment times (1 min and 15 min). After the placement of samples into the plasma chamber, the system was evacuated to a pressure of 20 mTorr. Then the oxygen gas was introduced to the system and oxygen flow rate was controlled in order to set the plasma pressure at the 20 mTorr. After setting pressure, discharge was applied and the treatment started. When the treatment time was over, the reactor was kept under oxygen atmosphere for 30 more minutes, to enhance remaining surface active radicals to react with oxygen. This also protected the surface against contamination that could have occurred when the reactor was opened to air.

2.4 Contact Angle Measurements

Contact angles were determined from the photos of 10 µL liquid droplets on the prepared and modified PMMA films by using a Windows Excel computer program. For statistical approach contact angles of at

least five drops of the same liquid were measured and the angles of the both sides of the drops were detected. Measurements, which had appeared unsymmetrical (when the difference between the angles of both sides were higher than five degrees), were excluded from the data. The temperature of the environment was kept constant at 20 ºC by air-conditioner.

2.5 Surface Free Energy Determination

The methods mentioned in the introduction part (Zisman, Saito, Fowkes, Berthelot, Geometric and Harmonic Mean and Acid-Base approaches) were used to find the SFE and its components. For this purpose Windows Excel program and Mathpad (Mark Widholm) program, working in the MAC OS environment, were used.

2.6 ESCA Characterizations

Electron Spectroscopy for Chemical Analysis (ESCA) spectra of the prepared and modified samples were acquired on a SPECS SAGE spectrometer (Germany) with a monochromatic Mg-K alpha radiation source (1253.6 eV). Base pressure was $1.3x10^{-9}$ mbar and a take-off angle of 90° with respect to the samples surface was used. The wide scan spectra for identification of elements were obtained over the range 0–1000 eV, using pass energy of 48 eV.

2.7 Cell Attachments and Proliferations

2.7.1 Cell Culture Studies

3T3 cells (passage 15) were cultivated in high glucose DMEM supplemented with 5 % fetal bovine serum FBS, 100 units/mL penicillin and 100 units/mL streptomycin at 37 ^{0}C in a carbon dioxide incubator (5 % CO_2, MCO-17AIC, Sanyo Electric Co. Ltd., Japan). The cells were passaged using 0.05 % trypsin-EDTA solution.

2.7.2 Cell Seeding

In the cell seeding tests untreated and plasma treated PMMA films which were prepared as described in section 2.2 and placed into plasma reactor in glass petri dishes were used. Films were sterilized by exposure to UV for 30 min. at room temperature and placed into 24-well plates.

3T3 cells were detached from the tissue culture flasks by using % 0.05 trypsin for 5 min at 37^0C, then centrifuged for 5 min at 3000 rpm and resuspended in high glucose DMEM supplemented with 5 % FBS, 100 units/mL penicillin and 100 units/mL streptomycin.

Cell number was counted using Nucleo Counter (ChemoMetec A/S, Denmark). 50 000 cells/20 μL were seeded on each film and the films were not disturbed for 30 min. to allow cell attachment. After 30 min, 500 μL high glucose DMEM supplemented with 5 % FBS, 100 units/mL penicillin and 100 units/mL streptomycin were added. They were incubated in a CO_2 incubator (5 % CO_2, 37 ^{0}C) for 1 day. Tissue culture polystyrene (TCPS) was used as the positive control.

2.7.3 Cell Proliferation

Cell number was quantified by using MTS assay (Nonradioactive cell proliferation assay [31].) A calibration curve was constructed using the predetermined cell numbers (counted with NucleoCounter) of 3T3 cells. For this purpose 25 000, 50 000, 100 000, 250 000 and 500 000 cells were seeded on 24 well plates in triplicate and incubated for 4 h. The medium was then removed and the sample was washed with PBS. Then MTS solution (500μL, 10 % PMS and MTS in DMEM low glucose medium) was added. After 2 h of incubation at 37 ^{0}C, 100 μL of this solution was transfered to a 96-well plate. The optical density (OD) at 490 nm was determined with a kinetic microplate reader (Maxline Vmax®, Molecular Devices, USA) and a plot of OD versus cell number was prepared as a calibration curve (Figure 2.2).

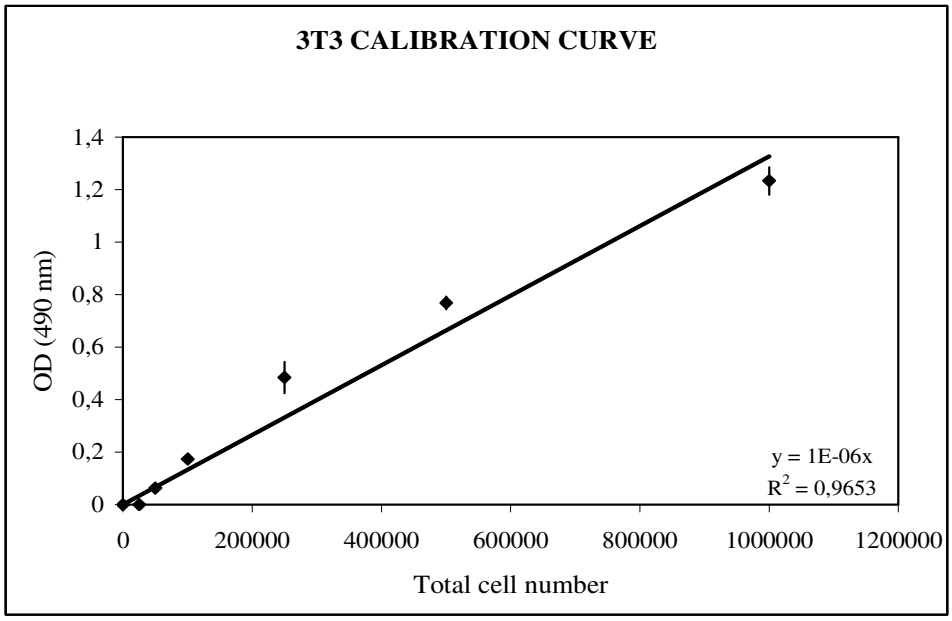

Figure 2.2 3T3 calibration curve obtained by MTS assay.

After seeding of the cells on the films, the cell numbers were quantified by using the calibration curve for 3T3 cells. For this purpose, the construct was transferred into a fresh 24-well plate, and was washed with PBS and MTS (500 μL) solution was added. The cells were incubated for 2 h in the CO_2 incubator and the OD at 490 nm of the aliquots from the wells was measured with kinetic microplate reader. The proliferation amounts for 3T3 cells seeded onto films were obtained.

2.7.4 Imaging of the Cells

Images of the cells were obtained by using fluorescence microscope (IX 70, Olympus, Japan). For this purpose, 3T3 cells seeded onto films were first fixed by glutaraldehyde (2.5 %) for 2 h and then washed twice with cacodylate buffer (0.1 M, pH 7.4). For staining of the cells, the samples were washed with HCl (0.1 M) for 1 min and then 500 μL of Acridine orange was added. After 15 min, Acridine orange was removed by drawing it back with the micro syringe and then by

washing samples with distilled water. The cells were observed under the fluorescence microscope at the excitation wavelength of 480 nm.

CHAPTER 3

RESULTS AND DISCUSSIONS

3.1 SFE Results For the Control Group (Untreated PMMA)

The untreated PMMA film's SFE and components were evaluated with different approaches. The results were compared to each other to elucidate the differences of methods with different notions and to find the useful liquid combinations for the calculations used for the pristine PMMA films. Results of different liquid pairs and triplets were compared to examine the effects of liquid types on the results.

3.1.1 Zisman and Saito Approaches

Contact angle values obtained from different drops of the same the liquid were quite precise. The precision can be seen from the small standard deviation numbers compared to average values given in Table 3.1. The relatively small standard deviation values of the contact angles also show the smoothness and homogeneity of the surfaces of the pristine PMMA films. By using these measured contact angle values Zisman and Saito plots were obtained. The linearity of the plots also showed precision of the contact angles (Diiodomethane and Bromonaphthalene were also used as test liquids however they were taken out of the Zisman's and Saito's plot because they did not fit in the graphics). SFE of PMMA obtained from Zisman plot (Figure 3.1) was 32.5 mJ/m^2 and Saito plot (Figure 3.2) was 36.7 mJ/m^2. The difference is about 4 mJ/m^2. Even though this is not a significantly large difference, the result of Saito plot was found to be closer to the results of other methods.

In spite of the likelihood that SFE and hydrophilicity are not directly related, Zisman plot implies the point below which the surface will be wetted completely and this gives a relation between SFE and

wettability, but does not give the real SFE. In addition, Zisman plot does not take the components of SFE into accounts. In the Zisman plot liquids are expected to be in trend with their total SFE. As a result, not all the liquids may fit the Zisman plot because the polar and non-polar characters of the liquids are not in trend with the total SFE. Diiodomethane and bromonapthalene were the two liquids in our test liquids to have almost zero polar components and PMMA also has an non-polar surface [29, 32, 33]. Consequently, they give lower contact angles than the values expected to be on the Zisman plot. On the other hand, water is the most polar liquid among the test fluids which were used in our study and it gives the highest contact angle value. However, water is also the liquid with highest total SFE among the test liquids, so it fits the Zisman plot by giving the highest contact angle value.

Table 3.1 Contact Angle values and their standard deviations obtained for different liquids.

Liquids (Abbreviations)	Average contact angle (θ)	Standard Deviation
Water (W)	63.51	0.86
Glycerol (G)	53.02	2.04
Formamide (F)	49.11	2.13
Diiodomethane (Dm)	32.46	2.01
Ethylene Glycol (E)	40.36	0.91
Bromonaphthalene (B)	26.63	1.33
Diethylene Glycol (De)	33.25	1.96
Dimethyl Sulfoxide (DMSO)	32.32	1.92
Tricresylphosphate (T)	25.84	1.73

When it is considered that Zisman plot gives better results for homologous series of liquids [7] and Zisman plot ignores the spreading pressure contributions to SFE [8], it is reasonable to think that the more accurate value of SFE of the pristine PMMA film comes from the Saito plot which resulted in 36.7 mJ/m^2.

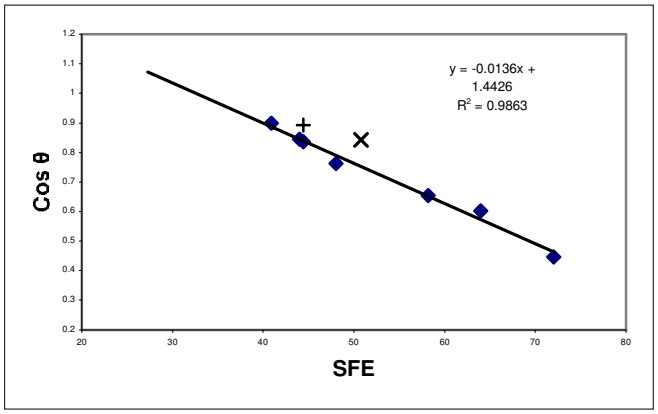

Figure 3.1 Zisman Plot (+ indicates bromonapthalene and x indicates diiodomethane)

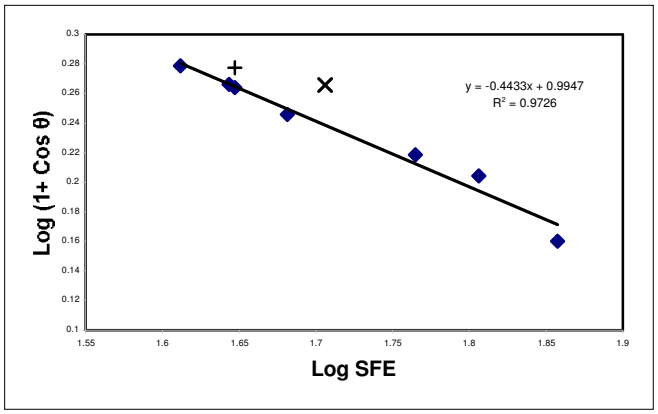

Figure 3.2 Saito Plot (+ indicates bromonapthalene and x indicates diiodomethane)

3.1.2 Geometric Mean Approach

Geometric mean equation was applied for all possible combinations of nine unlike test liquids to see the precision and accuracy. The test liquids data are given in Table 3.2 and the results for Geometric Mean equation are give in Table 3.3 and Table 3.4. Three of the combinations clearly deviated from other pairs. These were glycerol-ethyleneglycol, formamide-ethyleneglycol and formamide-diethyleneglycol. In these pairs' results, the polar and dispersive

components demonstrated high deviations on both directions. It is interesting to note that the total SFE values were all higher than the average value. For example G-E pair's outcomes as dispersive and polar components were found to be 3.95 and 52.53 mJ/m^2, respectively, and for the F-De pair these values were 8.57 and 46.43 mJ/m^2, while for F-E pair these values were in opposite direction and found as 43.88 and 2.30 mJ/m^2. For the same pairs of G-E, F-De and F-E the total SFE values were 56.48, 55.00 and 46.18 mJ/m^2 and all were higher than the average value of 40.04 mJ/m^2. The common property of these three liquids is that they all have hydroxyl groups as functional groups which may interact with the carbonyl groups of the PMMA surface. However this should not make them the cause of error since they gave in-range results with other combinations. On the other hand, the two being together and having the hydroxyl groups both may be the reason for such results.

In a previous study done by Shimizu and Demarquette [8] it was reported that, better results from Geometric or Harmonic Mean methods were obtained when a liquid combination was selected such that, the pair contained the most and the least polar fluids among the test liquids to be used in the equations. Based upon their findings, it may be assumed that in our study the most accurate results come from the water-formamide, water-diiodomethane, water-bromonaphthalene combinations since the polarity difference between these fluids are the greatest among all other pairs. The combination of water-formamide gave a result of 21.83 mJ/m^2 as a dispersive component and 18.61 mJ/m^2 as a polar component. These add up to give 40.44 mJ/m^2 for the total SFE. Even though the total SFE is close to the literature values of PMMA, the ratio of polar to dispersive component is too high in this pair's result when compared to literature. Normally PMMA in literature [29,32,33] is given as a highly non-polar polymer with a high ratio of dispersive component to polar component. For example in one study [33] the dispersive component to polar component ratio for PMMA was given as 33.1/10.4, which was obtained from the Geometric Mean

method. In another study [32] the ratio of dispersive to polar component of PMMA's SFE was found to be 35.00/0.26 and this was also estimated by the Geometric Mean method. Yet, in another study [29] the dispersive component of PMMA obtained from Acid-Base approach ranged between 28.8 to 118.1 mJ/m^2 and polar component ranged from 0.6 to 4.5 mJ/m^2. According to the authors of this study the most reliable outcome of their calculations gave a dispersive component value of 38.5 mJ/m^2 and a polar component value of 1.6 mJ/m^2 which gives a total of 40.1 mJ/m^2. As it can be seen, very large differences exist in the results and this points the inconsistency between the liquids used and the methods applied. Therefore, the choice of the liquids and the methods is not an easy decision for the calculation of SFE and components.

Table 3.2 Surface Tension values (mJ/m^2) and their dispersive and polar components of liquids used.

LIQUID	Symbols	γ_L^d	γ_L^p	γ_{Total}
Water*	W	21.8	51	72.8
Glycerol*	G	34	30	64
Formamide*	F	39.5	18.7	58.2
Diiodomethane [a]	Dm	44.1	6.7	50.8
Diiodomethane [b]	Dm	50.8	0	50.8
Ethylene Glycol*	E	29	19	48
Bromonaphthalene*	B	44.4	0	44.4
Diethylene Glycol*	De	31.7	12.7	44.4
Dimethyl Sulfoxide*	DMSO	36	8	44
Tricresylphosphate*	T	36.2	4.5	40.7

[a]from reference #8 ,[b]from reference #34, *from references #1,8,39

Table 3.3 Dispersive and polar components of SFE (mJ/m^2) of PMMA obtained from Geometric mean equation.

Liquid Couple	γ_S^d	γ_S^p	γ_{Total}
W–G	23.37	17.73	41.10
W–F	21.83	18.61	40.44
W–E	15.98	22.62	38.60
W–De	19.27	20.25	39.52
W–DMSO	22.62	18.15	40.77
W–T	25.52	16.74	42.26
G–F	21.63	19.40	41.03
G–E°	3.95	52.53	56.48
G–De	16.28	25.61	41.89
G–DMSO	22.34	18.71	41.05
G–T	25.58	15.78	41.36
F–E	43.88	2.30	46.18
F–De°	8.57	46.43	55.00
F–DMSO	23.54	16.47	40.01
F–T	26.80	13.30	40.10
E–De	25.49	11.97	37.46
E–DMSO	27.55	10.35	37.90
E–T	29.00	9.26	38.26
De–DMSO	28.94	8.65	37.59
De–T	30.00	7.74	37.74
DMSO–T	29.40	8.12	37.52
Average	25.21	14.83	40.04
Standard Deviation	6.11	5.94	2.19

°Excluded data

Table 3.4 Geometric mean results (mJ/m^2) with the couples containing the ones (Dm and B) being out of the ranges of Saito and Zisman plot.

Liquid Couple	γ_S^d	γ_S^p	γ_{Total}
Dm–W**	31.46	13.72	45.18
Dm–G**	33.87	9.99	43.86
Dm–F**	39.11	4.20	43.31
Dm–E**	39.79	3.64	43.43
Dm–B**	39.81	3.62	43.43
Dm–De**	45.57	0.59	46.16
Dm–DMSO**	NR	NR	NR
Dm–T**′°	0.25	282.66	282.91
B–W	39.82	10.52	50.34

Table 3.4 continued

B–G	39.82	6.97	46.78
B–F	39.82	3.88	43.70
B–E	39.82	3.63	43.45
B–De	39.82	0.38	40.20
B–DMSO	39.82	0.93	40.75
B–T	39.82	0.11	39.93
Dm–W*	43.17	9.45	52.63
Dm–G*	43.17	5.58	48.75
Dm–F*	43.17	2.55	45.72
Dm–E*	43.17	2.51	45.68
Dm–B*	NR	NR	NR
Dm–De*	43.17	1.12	44.29
Dm–DMSO*	43.17	0.17	43.34
Dm–T*	43.17	0.17	43.34
Average	40.53	4.19	44.71
Standard deviation	3.30	4.00	3.16

**Dm having γ^d = 44.10 and γ^p =6.70
*Dm having γ^d =50.8 and γ^p = 0
°Excluded data, NR: no solution from the equations

For PMMA, compared to W-F pair, W-Dm and W-B couples gave better results (Table 3.4) similar to literature with higher dispersive components and lower polar components. When we look at all the results on Table 3.4 it is seen that dispersive components are all found to be higher than polar components. In literature more than 3 different dispersive and polar components data exist for Dm [8,29,34]. In some studies Dm was accepted as a completely dispersive liquid. In the Table 3.4 the lowest (44.10 mJ/m^2) and highest (50.8 mJ/m^2) values of dispersive component of Dm obtained from the literature, [8,34] were used. The results of the Dm data with a polar component value of 6.7 mJ/m^2, gave dispersive component as 38.26 mJ/m^2, polar component as 5,86 and total SFE as 44.23 mJ/m^2 on the average while the Dm data with no polar component gave dispersive component as 43.17 mJ/m^2, polar component as 3.07 and total SFE as 46.25 mJ/m^2 on the average. On the other hand, an attention-grabbing observation in Table 3.4 is the precision of the dispersive component results when one of the pairs had zero polar component and also interestingly Dm and B

were the ones that did not fit the Zisman or Saito plots as explained in section 3.1.1. However these "out of range" liquids are in the pairs that gave the closest results to literature by giving the highest ratios of dispersive to polar components among all Geometric Mean solutions. Although polar-nonpolar liquid combinations gave the best results in other studies, in this study more accurate results were obtained as the polarities of the liquids in the pairs became closer and closer as given in Table 3.4.

Another interesting point is the results of E-De, E-DMSO, E-T, De-DMSO, De-T and DMSO-T at Table 3.3 which have close polarities and close values of total SFE and dispersive components (Table 3.2). The outcomes of these pairs are fair compared to other ones in the Table 3.3 even though they are not polar non-polar liquid combinations.

As mentioned in section 1.4.5 Geometric Mean method may also be applied by using all the liquids data at a time. The resulting plot is given in Figure 3.3. Application of all the test liquids together resulted in a polar component of 11.67 and a dispersive component of 30.30 resulting a total of 41.97 mJ/m^2 (Figure 3.3).

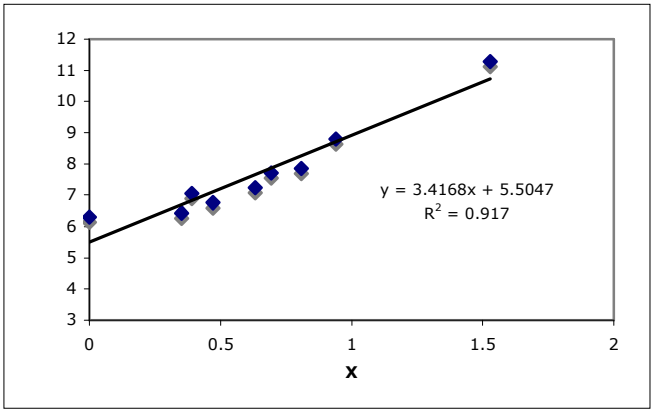

Figure 3.3 The plot of y (eqn. 12) vs x (eqn. 13) of equation 11 using all the test liquids data.

3.1.3 Berthelot's Approach

In Berthelot's Approach only total SFE is obtained by using different liquids which have various SFE values. When Berthelot's approach was applied and Cos θ vs 1/(SFE of liquids)^2 is plotted, Figure 3.4 is obtained. The total SFE of PMMA obtained from the plot was 30.60 mJ/m^2. The results obtained by use of single liquid values are given in Table 3.5. The results are relatively precise and accurate compared to other methods and to literature. The average SFE value is 38.9 mJ/m^2 and the standard deviation is ± 2.15.

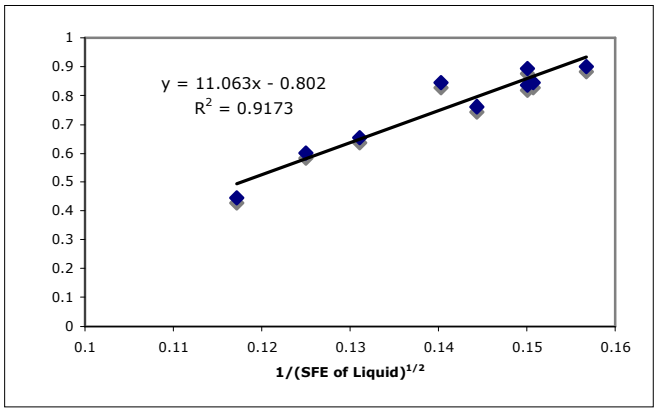

Figure 3.4 Application of data using Berthelot's Approach

Table 3.5 The results obtained from Berthelot's method using single liquids.

Liquid	Solid SFE
W	38.06
G	41.04
F	39.84
D	43.17
E	37.25
De	37.43
B	39.82
DMSO	37.44
T	36.73
Average	38.98
Standard deviation	2.15

3.1.4 Fowke's Approach

When Fowke's approach was applied only dispersive components can be calculated. The results did not show any consistency neither when the plot was used by taking all liquids into account nor when the values of single liquids were used. From the plot, the dispersive component of SFE was calculated as 7.39 mJ/m^2. The results obtained from single liquids are given in Table 3.6. Dispersive component of SFE are all higher than 40 mJ/m^2 except for bromonaphthalene which is 39.82 mJ/m^2. These results demonstrate that Fowke's approach is not applicable for PMMA surfaces. Since in literature total SFE for PMMA is given around 40 mJ/m^2 (29,32).

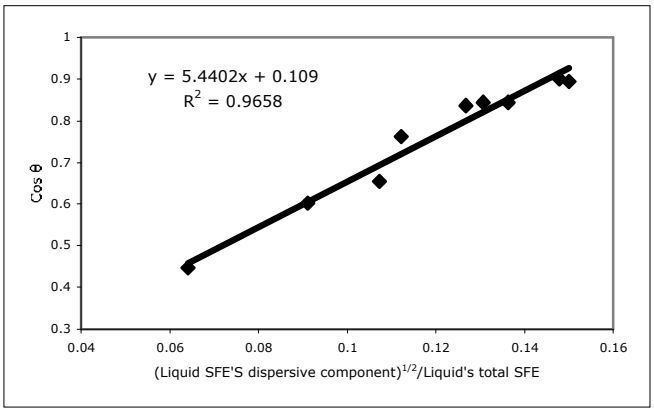

Figure 3.5 Application of data using Fowke's approach.

Table 3.6 The results obtained from Fowke's method using single liquids.

Liquid	Dispersive Component
W	127.09
G	77.25
F	59.45
D	49.73
E	61.66
De	52.42
B	39.82
DMSO	45.77
T	41.30
Average	61.61
Standard deviation	27.16

3.1.5 Harmonic Mean Approach

Harmonic Mean method appears to give quite different results than the Geometric Mean method. For all pairs, dispersive component values were found to be less than 40 mJ/m^2 (Table 3.7) The most accurate pair seems to be F-E in Table 3.7 since the highest dispersive to polar component ratio was obtained for this pair. Dm and B containing pairs gave better results (Table 3.8) when the polar component of the other liquid became smaller and closer to that of Dm or B's polar component.

Table 3.7 Dispersive and polar components of SFE of PMMA obtained from harmonic mean equation.

Liquid Couple	γ_S^d	γ_S^p	γ_{Total}
W-G	20.00	23.07	43.07
W-F	21.60	22.60	44.20
W-E	15.68	25.94	41.62
W-De	19.70	23.40	43.10
W-DMSO	24.30	20.92	45.22
W-T	27.60	19.60	47.20
G-F	23.00	19.70	42.70
G-E	12.00	37.95	49.95
G-De	19.70	23.41	43.11

Table 3.7 continued

G-DMSO	25.00	17.91	42.91
G-T	28.20	15.47	43.67
F-E	39.20	5.86	45.06
F-De	17.60	31.68	49.28
F-DMSO	26.00	14.84	40.84
F-T	28.70	12.70	41.40
E-De	24.80	13.16	37.96
E-DMSO	27.80	10.95	38.75
E-T	29.40	9.98	39.38
De-DMSO	29.20	8.76	37.96
De-T	30.20	8.02	38.22
DMSO-T	30.60	7.07	37.67
Average	24.78	17.76	42.54
Standard Deviation	6.10	8.37	3.57

NR: no solution from the equations

Table 3.8 Harmonic mean results with the couples containing Dm and B.

Liquid Couple	γ_S^d	γ_S^p	γ_{Total}
Dm-W**	32.00	17.85	49.85
Dm-G**	33.70	12.10	45.80
Dm-F**	36.60	6.96	43.56
Dm-E**	36.90	6.60	43.50
Dm-B**	39.93	3.89	43.82
Dm-De**	41.30	3.03	44.33
Dm-DMSO**	NR	NR	NR
Dm-T**	NR	NR	NR
B-W	39.93	16.05	55.98
B-G	39.93	9.58	49.51
B-F	39.93	5.49	45.42
B-E	39.93	5.63	45.56
B-De	39.93	3.45	43.38
B-DMSO	39.93	1.65	41.58
B-T	39.93	0.38	40.31
Dm-W*	43.44	15.35	58.79
Dm-G*	43.44	8.38	51.82
Dm-F*	43.44	4.20	47.64
Dm-E*	43.44	4.68	48.12
Dm-B*	NR	NR	NR
Dm-De*	43.44	2.45	45.89
Dm-DMSO*	43.44	0.66	44.10
Dm-T*	NR	NR	NR
Average	40.12	4.72	44.83
Standard deviation	2.80	3.20	2.42

**Dm having γ^d = 44.10 and γ^p =6.70
* Dm having γ^d =50.8 and γ^p = 0
NR: no solution from the equations

Up to this point, the results obtained from Geometric and Harmonic Mean methods, demonstrated large deviations and were significantly different from each other. These results create difficulty to find a relation between surface free energy, its components and biocompatibility. Deeper search of literature demonstrated similarly highly scattered results when more than two liquids were used in calculations. For instance in a study [8] values obtained from Harmonic Mean method for polypropylene surface deviated such that the results ranged from 7.23 to 34.5 mJ/m^2 for dispersive component of SFE and from 5.76 to 20.9 mJ/m^2 for polar component and from 23.7 to 40.3 mJ/m^2 for total SFE. For the same polypropylene the results obtained from Geometric Mean method were ranging from 7.43 to 40.6 mJ/m^2 for dispersive component, and from 0.392 to 11.8 mJ/m^2 for polar component and from 19.2 to 40.3 mJ/m^2 for total SFE. In the same study, calculations for other polymer surfaces also showed similar deviations depending on liquid couples and methods. In this mentioned study [8] 5 liquids (water, mercury, formamide, diiodomethane and ethyleneglycol) were used. However in our study nine liquids were used and all the possible combinations were estimated. So it is not illogical to obtain such a ranging data since SFE estimation depends on the choice of liquids and methods. The important point here is that; before studying on a certain surface one should try different methods and liquid combinations and see which ones are suitable for that particular surface. However, the science community still needs to improve SFE estimation methods and obtain approaches that would give precise results and would be in good agreement so that all the work would be simplified.

3.1.6 Acid-Base Approach

Before applying the acid-base approach we encountered with various values of test liquids' data available in the literature [4, 7, 29, 32]. Acidic and basic components of SFE of test liquids obtained from literature [29, 32] are given in Table 3.9. On the other hand the values

given by Della, Volpe and Siboni [4, 7, 29] are given in Table 3.10. The results obtained for PMMA by using these given data are demonstrated in Table 3.11 and 3.12, respectively. The results of components of SFE obtained by using Della, Volpe and Siboni values seem to be more acceptable since the average values and relative standard deviation values are more consistent.

Table 3.9 Acidic, basic components of surface free energies (mJ/m^2) of test liquids obtained from the literature [4, 32].

Liquid	γ_L	γ^{LW} (γ^d)	γ_L^-	γ_L^+	γ_L^{AB}
Water	72.8	21.8	25.5	25.5	51
Glycerol	64	34	57.4	3.92	30
Formamide	58	39	39.6	2.28	19
Diiodomethane	50.8	50.8	0	0	0
Ethylene Glycol	48	29	47	1.92	19
Bromonaphtalene	44.4	44.4	0	0	0
Dimethyl sulfoxide	44	36	32	0.5	8

Table 3.10 Acidic, basic components of surface free energies (mJ/m^2) of test liquids according to Della Volpe and Siboni [4,7,29].

Liquid	γ_L	γ^{LW} (γ^d)	γ_L^-	γ_L^+	γ_L^{AB}
Water	72.8	26.25	11.16	48.5	46.55
Glycerol	64	35.05	7.33	27.8	28.55
Formamide	58	35.5	11.3	11.3	22.5
Diiodomethane	50.8	50.8	0	0	0
Ethylene Glycol	48	33.9	51.6	0.97	14.1
Bromonaphtalene	44.4	44.4	0	0	0
Dimethyl sulfoxide	42.93	32.3	763	0.037	10.63

Table 3.11 data indicates that PMMA has a significant polar component with considerable acidic and basic components implying that it is bipolar. On the other hand Table 3.12 data shows a polymer with an almost completely dispersive character with a very small polar

character and almost monopolar since the acidic component is nearly zero. As a result Table 3.12 data fits more to the literature [29, 32] and it is quite reasonable. Acid base approach also gives deviations with different liquid triplets used. PMMA in literature is given as it mainly has a dispersive character. For instance in one study [32] use of W, Dm, B, E, F and G with acid base approach gave results ranging between 31.3 and 39.4 mJ/m^2 for dispersive component, between 0.69 and 684.03 mJ/m^2 for basic component, and between 0.04 and 48.83 mJ/m^2 for acidic component. In another study [29], the dispersive component of PMMA obtained from Acid-Base approach ranged between 28.8 to 118.1 mJ/m^2 while polar component ranged from 0.6 to 4.5 mJ/m^2. In this mentioned study, it was implied that the most reliable result of their calculations gave a dispersive component value of 38.5 mJ/m^2, a basic component of 3.6 mJ/m^2 and almost a zero acidic component meaning a surface with a monopolar character.

When data of triplets given in Table 3.12 is compared to each other, most deviations appear to occur when W-G or E-DMSO is present as a pair in the triplets. In the choice of liquid triplets it was suggested to use at least one completely dispersive liquid [4]. It can be said that, having one purely dispersive liquid (B or Dm) in the triplets demonstrated quite different results, bearing in mind W-G-Dm and W-G-B triplets did not achieve a solution and gave no results (Table 3.12).

Table 3.11 Surface free energy components (mJ/m^2) of PMMA surface calculated by acid-base approach using the liquid data given in literature (Table 3.9).

Liquid Triplets	γ_S	γ_S^{LW} (γ_S^d)	γ_S^-	γ_S^+	γ_S^{AB}
W-G-F	37.83	18.114	16.488	5.894	19.716
W-G-Dm	48.702	43.173	12.78	0.598	5.529
W-G-E	NR	NR	NR	NR	NR
W-G-B	46.783	39.818	13.174	0.921	6.965
W-G-DMSO	37.338	11.554	17.98	9.243	25.783
W-F-Dm	45.305	43.173	20.984	0.054	0.054
W-F-E	37.289	26.158	19.726	1.57	11.132
W-F-B	40.12	39.818	20.756	0.001	0.302
W-F-DMSO	NR	NR	NR	NR	NR
W-Dm-E	44.518	43.173	17.537	0.026	1.344
W-Dm-B	51.54	41.592	4.974	4.974	9.948
W-Dm-DMSO	NR	NR	NR	NR	NR
W-E-B	42.832	39.818	17.919	0.127	3.014
W-E-DMSO	36.718	24.166	20.036	1.966	12.551
W-B-DMSO	NR	NR	NR	NR	NR
G-F-Dm	NR	NR	NR	NR	NR
G-F-E	NR	NR	NR	NR	NR
G-F-B	NR	NR	NR	NR	NR
G-F-DMSO	41.063	20.237	43.393	2.499	20.826
G-Dm-E	NR	NR	NR	NR	NR
G-Dm-B	43.077	41.592	0.194	2.842	1.485
G-Dm-DMSO	NR	NR	NR	NR	NR
G-E-B	NR	NR	NR	NR	NR
G-E-DMSO	NR	NR	NR	NR	NR
G-B-DMSO	NR	NR	NR	NR	NR
F-Dm-E	45.677	43.173	6.796	0.231	2.503
F-Dm-B	42.237	41.592	0.077	1.344	0.645
F-Dm-DMSO	55.242	43.173	61.193	0.595	12.068
F-E-B	43.015	39.818	16.272	0.157	3.197
F-E-DMSO	35.603	32.612	53.464	0.042	2.991
F-B-DMSO	NR	NR	NR	NR	NR
Dm-E-B	42.045	41.592	0.046	1.122	0.453
Dm-E-DMSO	NR	NR	NR	NR	NR
Dm-B-DMSO	41.619	41.592	0.002	0.109	0.027
E-B-DMSO	NR	NR	NR	NR	NR
Average	43.095	35.234	18.605	1.969	7.861
Standard Deviation	5.199	11.100	20.875	2.720	8.836

NR: no solution for the equations

Table 3.12 Surface free energy components (mJ/m^2) of PMMA surface calculated by acid-base approach using the liquid data of Della Volpe and Siboni.

Liquid Triplets	γ_S	γ_S^{LW} (γ_S^d)	γ_S^-	γ_S^+	γ_S^{AB}
W-G-F	40.113	28.909	6.491	4.835	11.205
W-G-Dm	NR	NR	NR	NR	NR
W-G-E	36.267	30.016	9.2	1.062	6.251
W-G-B	NR	NR	NR	NR	NR
W-G-DMSO	32.553	30.748	11.218	0.073	1.805
W-F-Dm	44.206	43.173	7.918	0.034	1.032
W-F-E	41.643	39.28	7.486	0.186	2.363
W-F-B	41.714	39.818	7.546	0.119	1.896
W-F-DMSO	41.921	41.419	7.724	0.008	0.501
W-Dm-E	44.23	43.173	6.895	0.04	1.056
W-Dm-B	46.634	41.592	5.155	1.233	5.042
W-Dm-DMSO	43.513	43.173	7.257	0.004	0.34
W-E-B	41.991	39.818	7.423	0.159	2.173
W-E-DMSO	46.546	46.479	6.432	0	0.068
W-B-DMSO	40.479	39.818	8.182	0.013	0.661
G-F-Dm	45.623	43.173	4.103	0.366	2.45
G-F-E	NR	NR	NR	NR	NR
G-F-B	43.894	39.818	4.578	0.907	4.076
G-F-DMSO	NR	NR	NR	NR	NR
G-Dm-E	44.314	43.173	4.882	0.067	1.141
G-Dm-B	45.543	41.592	3.847	1.014	3.951
G-Dm-DMSO	43.477	43.173	5.329	0.004	0.303
G-E-B	41.947	39.818	5.797	0.195	2.129
G-E-DMSO	48.333	48.296	3.693	0.000	0.037
G-B-DMSO	40.423	39.818	6.627	0.014	0.605
F-Dm-E	44.288	43.173	5.75	0.054	1.115
F-Dm-B	45.641	41.592	2.025	2.025	4.049
F-Dm-DMSO	43.502	43.173	6.586	0.004	0.329
F-E-B	41.988	39.818	7.228	0.163	2.170
F-E-DMSO	48.111	48.084	3.971	0.000	0.027
F-B-DMSO	40.501	39.818	8.865	0.013	0.683
Dm-E-B	41.707	41.592	0.008	0.419	0.115
Dm-E-DMSO	43.587	43.173	13.563	0.003	0.414
Dm-B-DMSO	41.592	41.592	0.000	0.011	0.000
E-B-DMSO	40.810	39.818	23.944	0.010	0.992
Average	42.809	40.907	6.765	0.420	1.903
Standard deviation	3.194	4.340	4.242	0.948	2.357

NR: no solution for the equations

Up to this point, different approaches of SFE calculations were applied and compared to find the components of SFE for the prepared PMMA films. As it can be seen, from one approach to other and from one liquid to the other, all the values demonstrated quite large variations.

In literature, for the calculations of SFE of solids, generally 2 or 3 liquids with known SFE values are used and the results are given for these pairs or triplets only. In this study 9 different liquids were used and 5 different methods were applied to find SFE and its components and it was observed that it was not an easy process to find definite values for SFE and its components for a solid material.

3.2 SFE Results for the Modified PMMA

Application of plasma and modification of the surface chemistry of PMMA films changed the SFE and its components. The methods applied to control PMMA films were also applied to plasma treated films. Methods showed differences in the results, however, the total SFE was always found to be higher than that of the control group.

3.2.1 Results from the plots of Zisman and Saito

SFE results of plasma treated PMMA films obtained from Zisman and Saito plots are given in Table 3.13 and Table 3.14, respectively.

Table 3.13 SFE values of the plasma applied surfaces obtained from the Zisman Plot.

Plasma Application	SFE(mJ/m^2)
No Plasma (Control)	32,60
20 W for 1 min	40,83
100 W for 1 min	38,95
300 W for 1 min	37,03
20 W for 15 min	35,37
100 W for 15 min	40,34
300 W for 15 min	42,17

Table 3.14 SFE values of the plasma applied surfaces obtained from the Saito Plot.

Plasma Application	SFE(mJ/m^2)
No Plasma (Control)	36,70
20 W for 1 min	40,83
100 W for 1 min	40,75
300 W for 1 min	39,40
20 W for 15 min	38,38
100 W for 15 min	41,37
300 W for 15 min	43,17

It is clear that the plasma applications caused an increase in the total SFE values. According to Zisman plot results, for 1 min treatment, SFE first increased from 32.6 to 40.83 mJ/m^2 with application of 20 W power, but then decreased to 37.03 mJ/m^2 as the power was increased up to 300 W. The similar trend was also observed in Saito's results. On the other hand, when plasma application time was 15 min, a continuous increase up to 42.17 and 43.17 mJ/m^2 was observed in Zisman and Saito plots respectively, as the power was increased up to 300 W.

Even though, all plasma applications resulted in higher SFE than the control group, 15 minutes applications have parallel increase with rising power of plasma and generally 15 minutes applications resulted in higher SFE than 1 minute applications. Even though same trend was observed, Saito plots gave higher SFE values than Zisman plots' results.

It should be noted that Zisman and Saito do not give the real SFE but they imply the point below which the surface will be wetted completely and this gives a relation between SFE and wettability.

3.2.2 Results from the Geometric Mean Equation

SFE and its dispersive and polar components obtained from liquid couples with application of Geometric Mean Equation is given in Table 3.15 and Table 3.16.

Table 3.15 SFE and its components obtained from the geometric mean equation for different liquid couples used in measurements of 1 minute plasma applications.

Liquid Couple	Dispersive Component	Polar Component	Total
	20 W 1 MINUTE PLASMA		
W-G	20.30	34.53	54.83
W-F	27.37	29.18	56.56
W-Dm*	26.31	29.91	56.22
W-Dm	45.77	19.36	65.13
W-E	10.44	45.37	55.81
W-De	11.90	43.13	55.03
W-A	4.60	55.38	59.98
G-F	36.51	17.98	54.50
G-Dm*	28.09	25.29	53.38
G-Dm	45.77	12.05	57.82
G-E	0.03	110.12	110.15
G-De	6.81	62.31	69.12
G-A	NR	NR	NR
F-Dm*	25.58	31.94	57.52
F-Dm	45.77	10.28	56.04
F-E	NR	NR	NR
F-De	NR	NR	NR
F-A	NR	NR	NR
Dm-E*	35.50	11.16	46.66
Dm-E	45.77	5.49	51.26
Dm-De*	44.98	2.02	47.00
Dm-De	45.77	1.77	47.53
Dm-A*	37.70	8.27	45.96
Dm-A	45.77	4.68	50.45
E-De	14.58	35.81	50.39
E-A	74.10	0.01	74.11
De-A	23.80	18.57	42.37
	100 W 1 MINUTE PLASMA		
W-G	13.26	45.10	58.36
W-F	21.99	36.36	58.35
W-E	5.98	56.21	62.19
W-De	11.77	46.97	58.73
W-A	2.40	65.33	67.73
G-F	34.33	18.96	53.29
G-E	NR	NR	NR
G-De	10.64	50.67	61.31
G-A	NR	NR	NR
F-E	NR	NR	NR
F-De	NR	NR	NR
F-A	NR	NR	NR
E-De	25.94	17.86	43.80
E-A	47.29	4.09	51.38
De-A	30.11	12.98	43.10
	300 W 1 MINUTE PLASMA		
W-G	15.08	42.10	57.18
W-F	26.83	31.82	58.65
W-Dm*	23.91	34.00	57.91
W-Dm	44.53	21.76	66.29
W-De	11.47	46.43	57.89
W-A	2.79	62.98	65.77
G-F	43.89	12.75	56.64
G-Dm*	26.67	26.26	52.94
G-Dm	44.53	12.39	56.92
G-De	8.93	55.36	64.29
G-A	NR	NR	NR
F-Dm*	21.99	40.25	62.23
F-Dm	44.53	12.26	56.79
F-De	NR	NR	NR
7--F-A	NR	NR	NR
Dm-De*	39.70	4.88	44.58
Dm-De	44.53	2.63	47.16
Dm-A*	35.76	9.20	44.96

Table 3.15 continued

Dm-A	44.53	5.04	49.57
De-A	27.72	14.79	42.51

*Dm with a polar value was used, NR is put when equation gave no solution for the couple. (Abbreviations; W: Water, G: Glycerol, Dm: Diiodomethane, E: Ethylene Glycol, De: Diethylene Glycol A: Aniline).

Table 3.16 SFE and its components obtained from the geometric mean equation for different liquid couples used in measurements of 15 minutes plasma applications.

Liquid Couple	Dispersive Component	Polar Component	Total
	20 W 15 MINUTE PLASMA		
W-G	12.70	46.64	59.34
W-F	26.32	33.74	60.05
W-Dm*	24.50	35.12	59.62
W-Dm	45.75	22.47	68.22
W-E	5.40	58.42	63.82
W-De	10.46	49.67	60.13
W-A	2.11	67.46	69.57
G-F	47.23	10.97	58.20
G-Dm*	28.39	24.56	52.95
G-Dm	45.75	11.75	57.50
G-E	NR	NR	NR
G-De	8.81	55.76	64.58
G-A	NR	NR	NR
F-Dm*	23.28	39.00	62.28
F-Dm	45.75	12.02	57.77
F-E	NR	NR	NR
F-De	NR	NR	NR
F-A	NR	NR	NR
Dm-E*	37.19	8.88	46.07
Dm-E	45.75	4.65	50.41
Dm-De*	43.05	3.21	46.26
Dm-De	45.75	2.17	47.92
Dm-A*	37.64	8.32	45.96
Dm-A	45.75	4.71	50.46
E-De	22.79	21.31	44.10
E-A	44.07	5.35	49.41
De-A	26.90	15.72	42.61
	100 W 15 MINUTE PLASMA		
W-G	10.89	50.88	61.77
W-Dm*	25.22	36.08	61.30
W-Dm	47.07	23.09	70.16
W-E	8.01	55.36	63.37
W-De	10.86	50.91	61.77
W-A	1.38	72.61	74.00
G-Dm*	30.17	23.02	53.20
G-Dm	47.07	11.17	58.24
G-E	2.88	78.13	81.01
G-De	10.85	50.98	61.83
G-A	NR	NR	NR
Dm-E*	35.77	12.59	48.35
Dm-E	47.07	6.05	53.12
Dm-De*	44.13	3.42	47.55
Dm-De	47.07	2.26	49.33
Dm-A*	40.00	7.10	47.10
Dm-A	47.07	4.22	51.29
E-De	16.69	34.68	51.37
E-A	NR	NR	NR
De-A	31.53	12.05	43.59

Table 3.16 continued

	300 W 15 MINUTE PLASMA		
W–G	0.67	83.12	83.79
W–Dm*	39.86	39.86	79.72
W–Dm	49.69	25.43	75.11
W–De	8.62	59.77	68.39
G–Dm*	39.42	10.91	50.32
G–Dm	49.69	6.16	55.85
G–De	21.38	25.64	47.02
Dm–De*	51.02	1.18	52.20
Dm–De	49.69	1.52	51.21

*Dm with a polar value was used, NR is put when equation gave no solution for the couple.

Use of geometric mean equation resulted in a very wide range of values instead of one certain result as in the case of Zisman and Saito Plots. However, the general trend seems to show an increase in total SFE of the modified PMMA films. When all data is considered, the common liquid couples, which gave results in all plasma applications, are water-glycerol, glycerol-diethylene glycol and water-diethylene glycol. One point which can be emphasized here is that, the polar component is quite higher than the dispersive component, contrary to the untreated control group. Therefore, we can conclude that oxygen plasma created polar groups (such as carboxyl, hydroxyl etc.) on the surface causing an increase in the polar component value of SFE.

Shimuzu and Demarquette [8] previously showed that polar and non polar liquid combinations are most trustable when Geometric or Harmonic mean methods are used. Water-diethylene glycol pair is the one that has the highest polarity difference among these and the results of this pair seem to be in trend with the plasma applications.

In this work two different data of Dm was used. More than 3 different dispersive and polar components data exist in the literature [8,29,33]. The question is whether to accept Dm as a completely dispersive liquid or not. We used the ones having lowest and highest values of dispersive component of Dm; one having no polar component and the other having the most among the literature data (Table 3.17). It was interesting to observe that dispersive components gave the same values when Dm with no polar component was used and the dispersive

results were always lower when Dm with polar component was used. In this case the use of Dm value with polar component is more reliable since oxygen plasma is expected to increase the polarity of the surface with the introduction of new polar groups [35].

Table 3.17 Surface Tension values (mJ/m^2) and their dispersive and polar components of the test liquids used.

LIQUID	γ_L^d	γ_L^p	γ_{Total}
Water	21.8	51	72.8
Glycerol	34	30	64
Formamide	39.5	18.7	58.2
Diiodomethane [a]	44.1	6.7	50.8
Diiodomethane [b]	50.8	0	50.8
Ethylene Glycol	29	19	48
Bromonaphthalene	44.4	0	44.4
Diethylene Glycol	31.7	12.7	44.4
Dimethyl Sulfoxide	36	8	44
Tricresylphosphate	36.2	4.5	40.7

[a]from reference #33 ,[b]from reference #9

In addition, it should also be noted that water-diiodomethane could have been more suitable for the choice of pairs in the sense of polarity difference. But this was not the case in our study; diiodomethane seem to be interacting with the treated surfaces and this affects the contact angle values.

From water-diethylene glycol pair, it is seen that dispersive components do not tend to change much with the application of plasma but a slight decrease was observed (Figure 3.6). However when comparison is made to control group which is the untreated PMMA, there is a drastic decrease in dispersive component according to Geometric Mean calculations, while almost no change occurred according Harmonic Mean calculations. The value of dispersive component in the control group was 19.27 mJ/m^2 from the water–diethylene glycol couple.

Polar components on the other hand tend to increase with plasma applications as expected (Figure 3.7). When comparison is made with

the control group whose polar component value was 20.25 mJ/m^2 from the water–diethylene glycol couple, a significant increase up to 59.77 mJ/m^2 was observed.

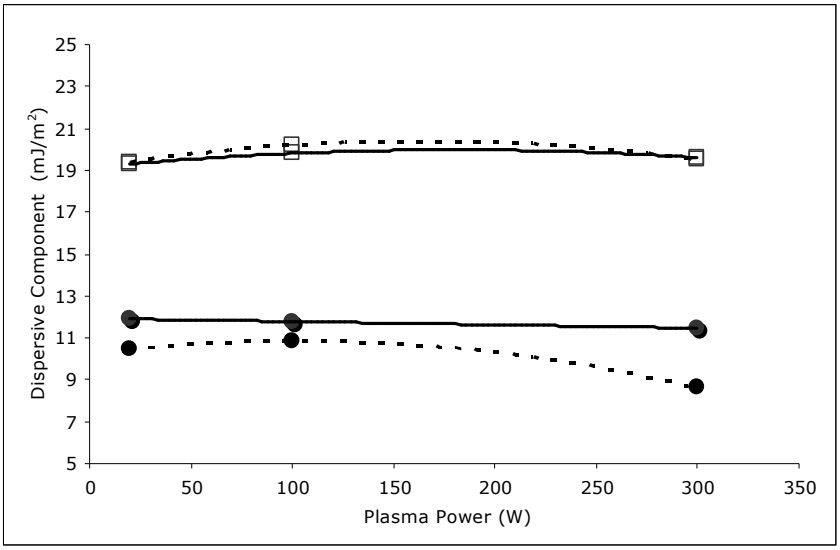

Figure 3.6 Dispersive components of SFE obtained by the geometric and harmonic mean equation from the water-diethylene glycol couple data vs plasma power. Continuous lines indicate 1 minute applications and disconnected ones indicate 15 minutes applications. ● Geometric mean results, ◘ Harmonic mean results.

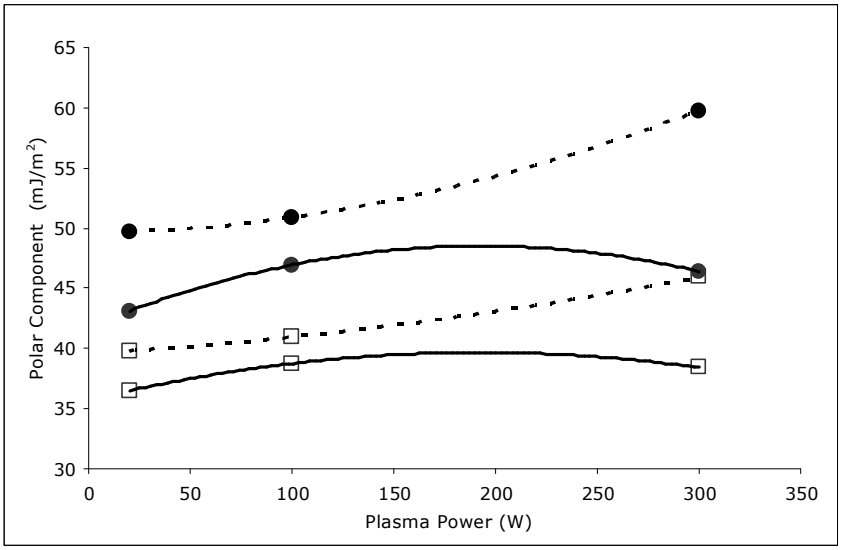

Figure 3.7 Polar Components of SFE obtained by the geometric and harmonic mean equation from the water-diethylene glycol couple data vs plasma power. Continuous lines indicate 1 minute applications and disconnected ones indicate 15 minutes applications. ● Geometric mean results, ◘ Harmonic mean results.

The total SFE also increased in the same trend with the application of plasma (Figure 3.8). Again the 15 minute applications of plasma are more effective than 1 minute applications. They resulted higher and correspondingly increasing SFE with plasma applications compared to 1 minute applications. This trend was also seen in the Zisman and Saito plots. The total SFE of the control group obtained from the geometric mean equation by the use of water-diethylene glycol couple was 39.52 mJ/m^2.

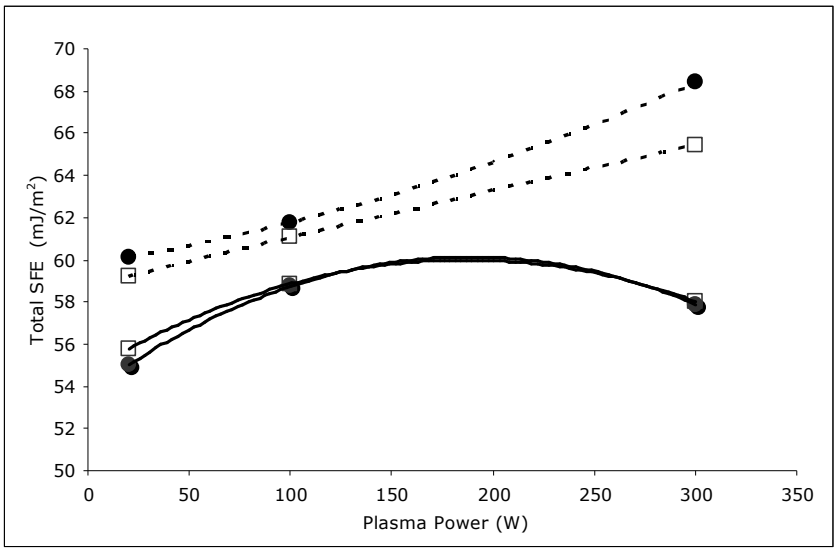

Figure 3.8 Total SFE obtained by the geometric and harmonic mean equation from the water-diethylene glycol couple data vs plasma power. Continuous lines indicate 1 minute applications and disconnected ones indicate 15 minutes applications. ● Geometric mean results, ◘ Harmonic mean results.

3.2.3 Results from the Harmonic Mean Equation

Results for SFE and its components obtained from the harmonic mean equation for different liquid couples used in measurements of 1 minute plasma applied samples are given in Table 3.18 and measurements of 15 minutes plasma applied samples are given Table 3.19.

Table 3.18 SFE and its components for 1 min. plasma applied surfaces calculated by the harmonic mean equation.

Liquid Couple	Dispersive Component	Polar Component	Total
	20 W 1 MINUTE PLASMA		
W-G	21.30	34.93	56.23
W-F	28.10	30.86	58.96
W-Dm*	32.40	28.96	61.36
W-Dm	45.89	24.89	70.77
W-E	16.60	38.94	55.54
W-De	19.30	36.48	55.78
W-A	12.40	43.93	56.33
G-F	34.00	20.65	54.65
G-Dm*	33.50	21.01	54.51
G-Dm	45.89	14.34	60.22
G-E	13.00	58.47	71.47
G-De	18.70	40.13	58.83
G-A	NR	NR	NR
F-Dm*	33.40	21.65	55.05
F-Dm	45.89	24.89	70.77
F-E	76.00	2.66	78.66
F-De	NR	NR	NR
F-A	65.00	4.65	69.65
Dm-E*	36.10	11.69	47.79
Dm-E	45.89	7.85	53.73
Dm-De*	41.20	4.84	46.04
Dm-De	45.89	3.37	49.26
Dm-A*	36.60	10.62	47.22
Dm-A	45.89	7.74	53.63
E-De	21.90	25.28	47.18
E-A	47.80	7.30	55.10
De-A	25.60	16.89	42.49
	100 W 1 MINUTE PLASMA		
W-G	17.90	40.75	58.65
W-F	25.70	34.80	60.50
W-E	14.30	44.78	59.08
W-De	20.10	38.76	58.86
W-A	11.40	49.02	60.42
G-F	33.00	20.74	53.74
G-E	NR	NR	NR
G-De	11.70	62.81	74.51
G-A	NR	NR	NR
F-E	NR	NR	NR
F-De	NR	NR	NR
F-A	NR	NR	NR
E-De	27.30	16.61	43.91
E-A	36.00	10.74	46.74
De-A	29.00	14.29	43.29
	300 W 1 MINUTE PLASMA		
W-G	18.90	39.04	57.94
W-F	28.50	32.59	61.09
W-Dm*	31.20	31.32	62.52
W-Dm	44.71	26.83	71.54
W-De	19.60	38.43	58.03
W-A	11.60	47.76	59.36
G-F	38.40	17.52	55.92
G-Dm*	32.40	21.44	53.84
G-Dm	44.71	14.51	59.22
G-De	19.90	36.87	56.77
G-A	6.90	105.49	112.39
F-Dm*	31.70	26.02	57.72
F-Dm	44.71	12.77	57.48
F-De	NR	NR	NR
F-A	72.20	3.77	75.97
Dm-De*	38.00	6.78	44.78
Dm-De	44.71	4.15	48.86

Table 3.18 continued

Dm-A*	35.40	10.86	46.26
Dm-A	44.71	7.92	52.63
De-A	27.70	15.07	42.77

*Dm with a polar value was used, NR is put when equation gave no solution for the couple.

Table 3.19 SFE and its components for 15 min. plasma applied surfaces calculated by the harmonic mean equation.

Liquid Couple	Dispersive Component	Polar Component	Total
	20 W 15 MINUTE PLASMA		
W-G	17.80	41.62	59.42
W-F	28.60	33.85	62.45
W-Dm*	32.00	32.23	64.23
W-Dm	45.87	27.67	73.54
W-E	14.10	45.78	59.88
W-De	19.40	39.82	59.22
W-A	11.30	50.21	61.51
G-F	40.40	16.51	56.91
G-Dm*	33.50	20.65	54.15
G-Dm	45.87	14.07	59.94
G-E	11.50	64.56	76.06
G-De	19.90	36.75	56.65
G-A	7.10	103.52	110.62
F-Dm*	32.80	25.36	58.16
F-Dm	45.87	12.66	58.53
F-E	107.00	0.10	107.10
F-De	NR	NR	NR
F-A	75.00	3.59	78.59
Dm-E*	36.70	10.40	47.10
Dm-E	45.87	7.06	52.93
Dm-De*	40.10	5.78	45.88
Dm-De	45.87	3.79	49.66
Dm-A*	36.60	10.59	47.19
Dm-A	45.87	7.76	53.63
E-De	25.70	18.17	43.87
E-A	34.00	11.76	45.76
De-A	27.30	15.58	42.88
	100 W 15 MINUTE PLASMA		
W-G	16.90	44.11	61.01
W-Dm*	33.10	32.99	66.09
W-Dm	47.13	28.46	75.60
W-E	16.50	44.56	61.06
W-De	20.10	40.96	61.06
W-A	10.90	52.66	63.56
G-Dm*	34.80	19.88	54.68
G-Dm	47.13	13.70	60.83
G-E	16.10	46.46	62.56
G-De	21.20	34.74	55.94
G-A	7.03	104.94	111.97
Dm-E*	36.80	12.72	49.52
Dm-E	47.13	8.52	55.65
Dm-De*	41.00	6.14	47.14
Dm-De	47.13	4.00	51.13
Dm-A*	38.10	9.98	48.08
Dm-A	47.12	7.44	54.56
E-De	23.80	24.81	6.00
E-A	69.30	4.13	73.43
De-A	29.90	13.77	43.67
	300 W 15 MINUTE PLASMA		
W-G	8.90	62.78	71.68
W-Dm*	34.90	35.82	70.72

Table 3.19 continued

W–Dm	49.69	31.07	80.77
W–De	19.50	45.94	65.44
G–Dm*	38.90	13.28	52.18
G–Dm	49.69	9.41	59.10
G–De	24.50	23.29	47.79
Dm–De*	46.00	4.26	50.26
Dm–De	49.69	3.41	53.10

*Dm with a polar value was used, NR is put when equation gave no solution for the couple.

Harmonic mean results are parallel to the geometric equation results in the sense that they demonstrated wide range of results in parallel trend with plasma applications. However the results were not close to the ones obtained from geometric mean calculations. The most parallel results are again seen in water-diethylene glycol pair. Harmonic mean equation resulted in higher dispersive components where as the polar components were quite lower. It can be concluded that the effect of plasma is more dominant in effecting the SFE of PMMA in 15 minute plasma applications.

3.2.4 Acidic Basic Components

The results for SFE and its acidic and basic components obtained from the acid base approach were given in Table 3.20. The liquid data used for the results in this table were obtained from data in Table 3.10.

Table 3.20 SFE and its acidic and basic components (mJ/m^2) obtained from the acid base approach using the liquid data of Della Volpe and Siboni.

Liquid Triplets	γ_S	$\gamma_S^{LW}(\gamma_S^d)$	γ_S^-	γ_S^+	γ_S^{AB}
		300 W 15 MIN			
W–G–Dm	NR	NR	NR	NR	NR
		100 W 15 MIN			
W–G–Dm	NR	NR	NR	NR	NR
W–G–E	45.03	13.73	29.31	8.35	31.30
W–Dm–E	51.26	47.07	18.00	0.24	4.19
G–Dm–E	51.06	47.07	9.10	0.44	3.99
		20 W 15 MIN			
W–G–F	60.18	12.86	9.72	57.59	47.32
W–G–Dm	NR	NR	NR	NR	NR
W–G–E	41.47	16.32	27.90	5.67	25.15
W–F–Dm	55.34	45.75	14.57	1.58	9.59
W–F–E	NR	NR	NR	NR	NR
W–Dm–E	48.42	45.75	18.24	0.10	2.66
G–F–Dm	57.31	45.75	2.99	11.19	11.56
G–F–E	NR	NR	NR	NR	NR
G–Dm–E	48.69	45.75	10.31	0.21	2.94
F–Dm–E	48.02	45.75	23.42	0.06	2.26
		300 W 1 MIN			
W–G–F	57.52	15.99	9.35	46.14	41.53
W–G–Dm	NR	NR	NR	NR	NR
W–F–Dm	55.20	44.53	13.29	2.14	10.67
G–F–Dm	56.70	44.53	3.57	10.38	12.17
		100 W 1 MIN			
W–G–F	58.73	14.26	13.37	39.96	44.47
W–G–E	41.13	17.01	26.79	5.43	24.12
W–F–E	48.72	46.22	17.50	0.09	2.50
G–F–E	NR	NR	NR	NR	NR
		20 W 1 MIN			
W–G–F	54.45	23.27	9.18	26.48	31.18
W–G–Dm	NR	NR	NR	NR	NR
W–G–E	41.65	26.23	19.78	3.00	15.42
W–F–Dm	54.59	45.76	11.95	1.63	8.83
W–F–E	NR	NR	NR	NR	NR
W–Dm–E	49.48	45.76	14.73	0.24	3.72
G–F–Dm	56.90	45.76	4.76	6.52	11.14
G–F–E	NR	NR	NR	NR	NR
G–Dm–E	49.42	45.76	10.23	0.33	3.66
F–Dm–E	49.38	45.76	18.62	0.18	3.62

Since most of the liquids spread over the films after plasma application, the liquid combinations to be used in the equations were much less. No common liquid triplet was obtained from the outcomes of acid-base equations in all plasma applications. Because of this, it was not possible to compare all the plasma treated samples. However, generally, the results seem to show that the plasma applied surfaces have more non-polar character than polar. This is not in agreement with the geometric

mean and harmonic mean equations' results. The control group gave solutions of many triplets and the average values for total SFE was 42,81 mJ/m^2, dispersive component was 40,91 mJ/m^2, acidic basic (polar) component was 1,90 mJ/m^2, acidic component was 0,42 mJ/m^2, and basic component was 6,77 mJ/m^2 which was obtained from the liquids data gathered from Della Volpe and Siboni [7,29]. Considering that oxygen plasma increases hydrophilicity and the oxygen content and introduces new polar groups, geometric and harmonic mean results seem more reliable.

The acidic and basic components of liquids have different data available in the literature aside from Della Volpe and Siboni's data. These literature [4, 32] data were also used in calculations and their results are given in the Table 3.21. The ones that gave no solution were indicated as NR in the table.

Table 3.21 SFE and its acidic and basic components (mJ/m^2) obtained from the acid base approach using the liquid data given in literature (Table 3.9).

Liquid Triplets	γ_S	$\gamma_S^{LW}(\gamma_S^d)$	γ_S^-	γ_S^+	γ_S^{AB}
		300 W 15 MIN			
W-G-Dm	NR	NR	NR	NR	NR
		100 W 15 MIN			
W-G-Dm	57.35	47.07	35.14	0.75	10.28
W-G-E	NR	NR	NR	NR	NR
W-Dm-E	50.21	47.07	42.98	0.06	3.14
G-Dm-E	NR	NR	NR	NR	NR
		20 W 15 MIN			
W-G-F	58.05	48.54	32.24	0.70	9.51
W-G-Dm	57.00	45.75	32.73	0.97	11.24
W-G-E	NR	NR	NR	NR	NR
W-F-Dm	57.57	45.75	32.03	1.09	11.81
W-F-E	NR	NR	NR	NR	NR
W-Dm-E	46.03	45.75	44.66	0.00	0.28
G-F-Dm	56.77	45.75	12.67	2.40	11.02
G-F-E	NR	NR	NR	NR	NR
G-Dm-E	NR	NR	NR	NR	NR
F-Dm-E	NR	NR	NR	NR	NR
		300 W 1 MIN			
W-G-F	56.68	44.44	30.12	1.24	12.24
W-G-Dm	56.72	44.53	30.10	1.23	12.19
W-F-Dm	56.70	44.53	30.12	2.14	12.17
G-F-Dm	56.67	44.53	30.87	1.19	12.14
		100 W 1 MIN			
W-G-F	53.18	33.95	33.94	2.72	19.23
W-G-E	NR	NR	NR	NR	NR
W-F-E	NR	NR	NR	NR	NR
G-F-E	NR	NR	NR	NR	NR
		20 W 1 MIN			
W-G-F	53.95	35.58	26.97	3.13	18.37
W-G-Dm	57.79	45.77	25.25	1.43	12.03
W-G-E	NR	NR	NR	NR	NR
W-F-Dm	55.85	45.77	27.71	0.92	10.08
W-F-E	NR	NR	NR	NR	NR
W-Dm-E	49.23	45.77	35.16	0.09	3.46
G-F-Dm	NR	NR	NR	NR	NR
G-F-E	NR	NR	NR	NR	NR
G-Dm-E	NR	NR	NR	NR	NR
F-Dm-E	NR	NR	NR	NR	NR

Acidic and basic components account for hydrogen bonding and Π electrons [36] and the plasma causes random changes on the surface by forming new functional groups and radicals. As a result these random changes might have caused random changes in the acidic basic components. Consequently acid base approach after plasma may give deviated results. So maybe it is more convenient to take dispersive and

polar components alone into account by geometric or harmonic mean equations when plasma treated surfaces are to be measured.

3.2.5 Hydrophilicity Change

Hydrophlicity of the films changed with the applied plasma. Mainly increasing the power or time of plasma treatment increased the hydrophilicity. Increase in hydrophilicty was observed more in 15 minute treatments. This can be seen with the decrease of water contact angle in Table 3.22.

Table 3.22 Contact angle values of the liquids used for determination of SFE before and after different plasma applications.

1minute	Contact Angle							
Plasma Application	W	G	F	Dm	E	De	A	T
CONTROL	63.5	NC	48.8	28.8	40.4	33.3	NC	25.8
20 W 1 min	43.0	34.2	20.2	26.1	19.3	21.7	9.0	NC
100 W 1 min	38.3	35.6	23.6	NC	24.4	14.0	10.0	NC
300 W 1 min	39.5	35.1	15.6	29.2	NC	17.7	10.6	NC
15 minutes	Contact Angle							
Plasma Application	W	G	F	Dm	E	De	A	T
CONTROL	63.5	NR	48.8	28.8	40.4	33.3	NC	25.8
5W 15 min	57.8	49.3	45.1	34.3	42.7	38.0	8.6	NC
20 W 15 min	37.1	35.0	12.1	26.1	24.6	17.9	8.6	NC
100 W 15 min	34.6	34.7	*	22.3	9.5	11.0	9.0	NC
300 W 15 min	26.7	44.8	*	12.0	NC	9.7	NC	NC

*Angle below or around five degrees, NC stand for no contact angle

It is noteworthy to mention that hydrophilicity gave out the same trend as the variation of SFE and its polar components, which were mentioned in the previous sections, followed. It was seen that hydrophilicity is affected more by the polar component than the dispersive component.

3.2.6 Contact Angle Changes

As mentioned before, diiodomethane seem to interact with PMMA surface since it did not give appropriate contact angles and did not fit in the Zisman and Saito plots mostly. As a result diiodomethane was excluded from the control plot and most of plasma treated sample's

plots. Aniline on the other hand, completely wetted the surface of the untreated PMMA so it also was excluded. However it gave measurable contact angle values after plasma treatments**.**

Formamide, on the other hand, fits the plot for the untreated PMMA. However, when plasma is applied it deviated. It gave contact angles lower than the expected value in the plot. This may be due its nitrogen and oxygen content in the polar groups. When oxygen plasma is applied the oxygen content of the surface and its polar groups also increase [16, 35] and this might have caused an interaction between formamide and the surface.

3.3 Cell Attachment Results

Cell attachment tests were carried out for the samples modified with application of 15 minute plasma since the effect of modification was significant and more evident compared to the samples modified with 1 minute plasma applications. The average cell numbers attached to these surfaces are given in Figure 3.9 and 3.10. The average number of cells attached on the control group found as 18666 while this value increased up to 162333 for the modified surfaces with 100 W power application.

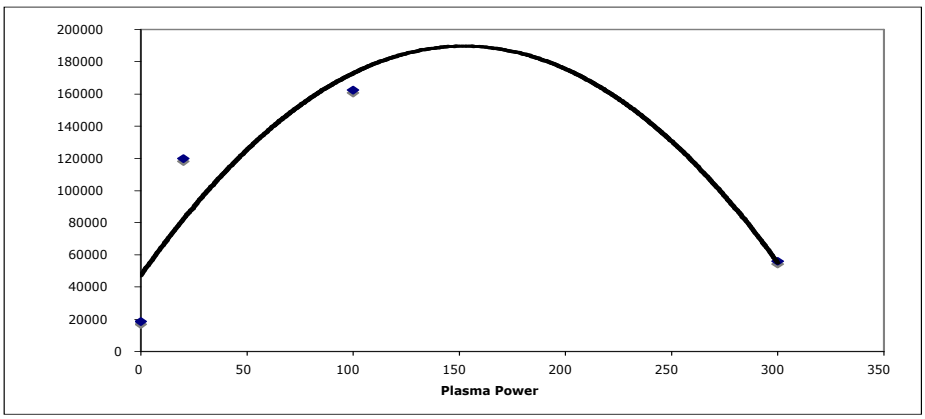

Figure 3.9 Average cell number vs plasma power which was applied for 15 minutes.

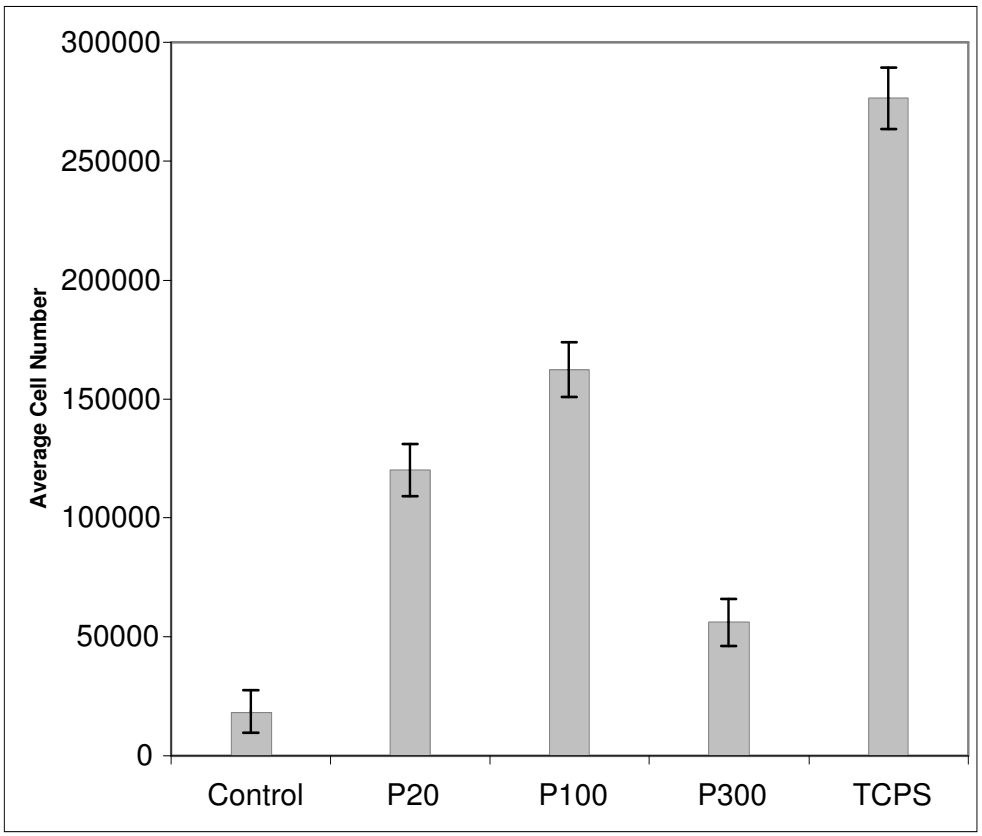

Figure 3.10 Average cell number versus plasma application graph graph including the TCPS. P20 is the plasma treatment of 20 W, P100 is the plasma treatment of 100 W and P300 is the plasma treatment of 300 W. For all samples the duration of plasma application was constant at 15 min.

Actually for all surfaces modified with plasma, whatever the SFE change was, the number of attached cells increased at least three times. Even for the samples modified with 20 W, the number of attached cells increased about 6 times. All the modified and control PMMA surfaces had lower numbers of attached cells compared to tissue culture dish made of polystyrene (TCPS). Numbers of cells attached on the pristine and modified films are given in Table 3.23.

Table 3.23 Cell attachment results on the prepared and modified PMMA and TCPS.

Sample	Average Cell Number*	Standard Deviations
Control	$1.9*10^4$	$0.9*10^4$
P-20	$1.2*10^5$	$1.1*10^4$
P-100	$1.6*10^5$	$1.2*10^4$
P-300	$5.6*10^4$	$0.1*10^4$
TCPS	$2.7*10^5$	$1.5*10^4$

*Plasma was applied for 15 minutes

Cell attachment did not show a parallel increase neither with the total SFE nor with the components. The dispersive component does not have the dominant effect on the cell attachment since it stayed almost steady during plasma treatments. However the total SFE and polar component values increased but the cell attachment did not follow the same trend. Cell attachment values dropped for the surfaces modified with 300W application but it was still higher than that of the control group. The samples modified with 100W plasma application achieved the highest cell attachment among the samples.

The common liquid pair in our calculations for Geometric Mean method was W-De couple. This couple's results for dispersive component did not change much and stayed around 10 mJ/m^2 where as polar component changed from 49.67 to 50.91 and to 59.77 mJ/m^2 with the application of 20 W to 100 W and to 300 W plasma respectively. The total SFE change was 60.13 to 61.77 and to 68.39 mJ/m^2. As a result it was seen that a polar component value of 50.91 mJ/m^2 and a total SFE of 61.77 mJ/m^2 corresponded to highest cell attachment. The common liquid pair from the Harmonic Mean method was again W-De couple. This pair's results for dispersive component from Harmonic Mean also did not change much and but stayed around 20 mJ/m^2 this time. On the other hand, polar component changed from 39.82 to 40.96 and to 45.94 mJ/m^2 with the application of 20 W to 100 W and to 300 W plasma respectively. The total SFE change was 59.22 to 61.06 and to 65.44 mJ/m^2. Consequently, this time, a polar component value of

40.96 mJ/m^2 and a total SFE of 61.06 mJ/m^2 corresponded to highest cell attachment from Harmonic Mean method. Both methods indicated a total SFE around 61 mJ/m^2 at the highest cell attachment however polar values differ by 10 mJ/m^2. Since the dispersive component stayed steady in both methods with plasma, it could be concluded that dispersive component was not the dominant parameter.

The cells attached on the films were labeled by fluorescence and photographs were taken by fluorescence microscope (IX 70, Olympus). The obtained cell images are given in Figure 3.11-3.14. It is not possible to find a definite number and compare the attachments just by looking at the images since cells were mostly layered. However the pictures show that the cells were attached to the surfaces and the untreated PMMA demonstrated the lowest value and it was really behind the modified surfaces in terms of cell attachment.

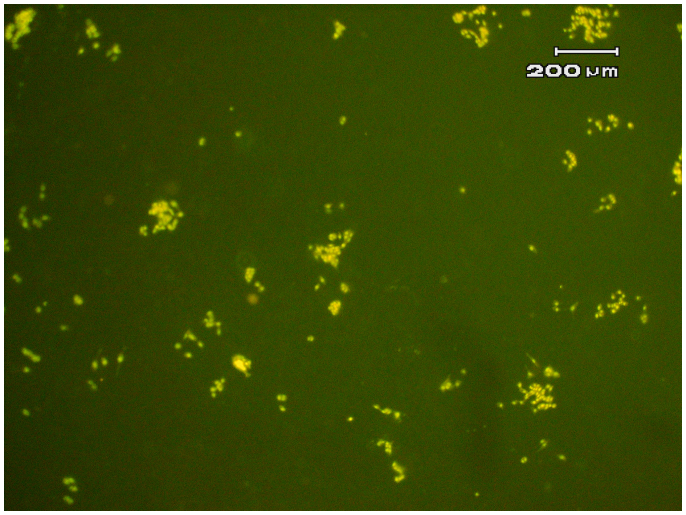

Figure 3.11 Attached cells on the control group.

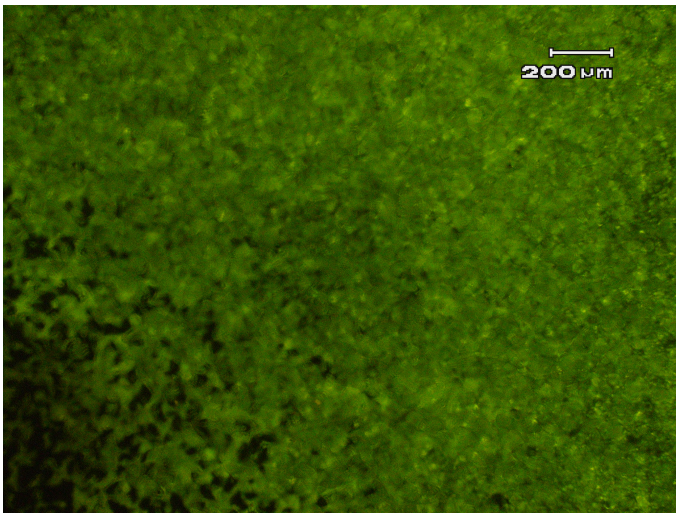

Figure 3.12 Attached cells on the 20 W 15 minute plasma applied PMMA surface.

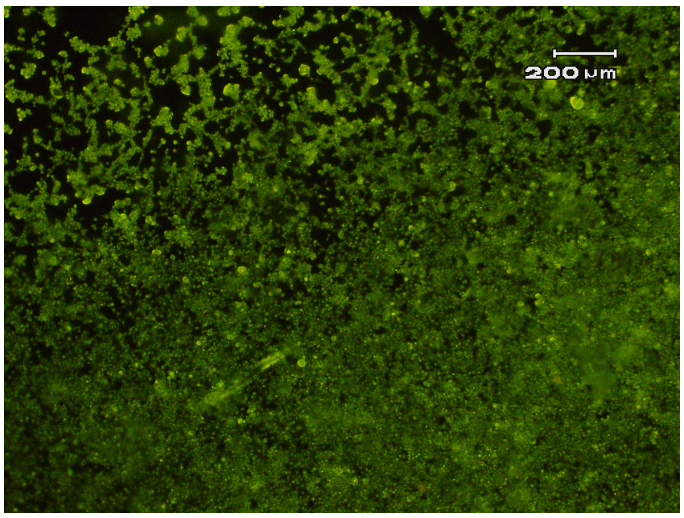

Figure 3.13 Attached cells on the 100 W 15 minute plasma applied PMMA surface.

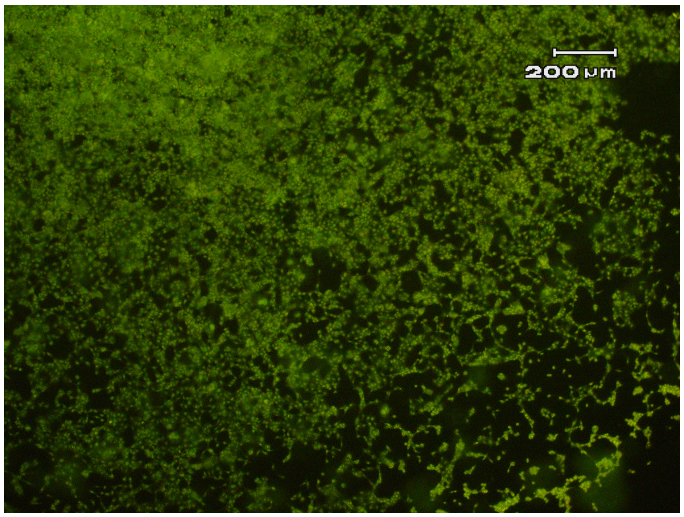

Figure 3.14 Attached cells on the 300 W 15 minute plasma applied PMMA surface.

Achievement of better cell attachments, on the surfaces of PMMA modified by plasma is important when conditions like cell attachment is needed at the surface but not in the bulk. For instance in ophthalmology, when an implant is replaced for the cornea, material needs to allow cell attachment at the surface but not at the interior parts of the material for the sake of implant's longevity [27]. The advantage of plasma is seen here with its alteration of the surface without affecting the bulk because plasma causes changes only at a few molecular level. So cells are attached to the surface but can not diffuse down to the interior. Even if they diffuse the attachment would be as low as the untreated PMMA.

Since plasma only made changes at very short molecular levels, hydrophilicity and work of adhesion properties of the whole material was changed by plasma applications owing to the fact that intermolecular forces that were responsible for these properties are short ranged. So the unchanged properties of molecules below the modified layers did not exhibit their original properties in terms of hydrophilicity and work of adhesion.

Cell attachment results were not in a parallel trend with hydrophilicity and oxygen content changes. As mentioned previously, cell attachment decreased with 300 W plasma application even though hydrophilicity kept increasing. Also 300 W and 100 W plasma applied surfaces' oxygen content were almost same but cell attachment results were quite different. These show that there is a critical hydrophilicity value for the attachment of the cells. Above and below this value the number of attached cells decreases.

Up to 100 W treatment, oxygen increase was in trend with plasma power. However, with the application of 300 W plasma, oxygen content did not change compared to the previous plasma application (100 W) and even became a little lower. Results are given in Table 3.24 and ESCA graphs are shown in Figures 3.15-3.18.

Table 3.24 Oxygen content change with plasma application of 15 min.

Sample	Oxygen Percentage
Control	27.0
P-20	30.0
P-100	34.3
P-300	34.0

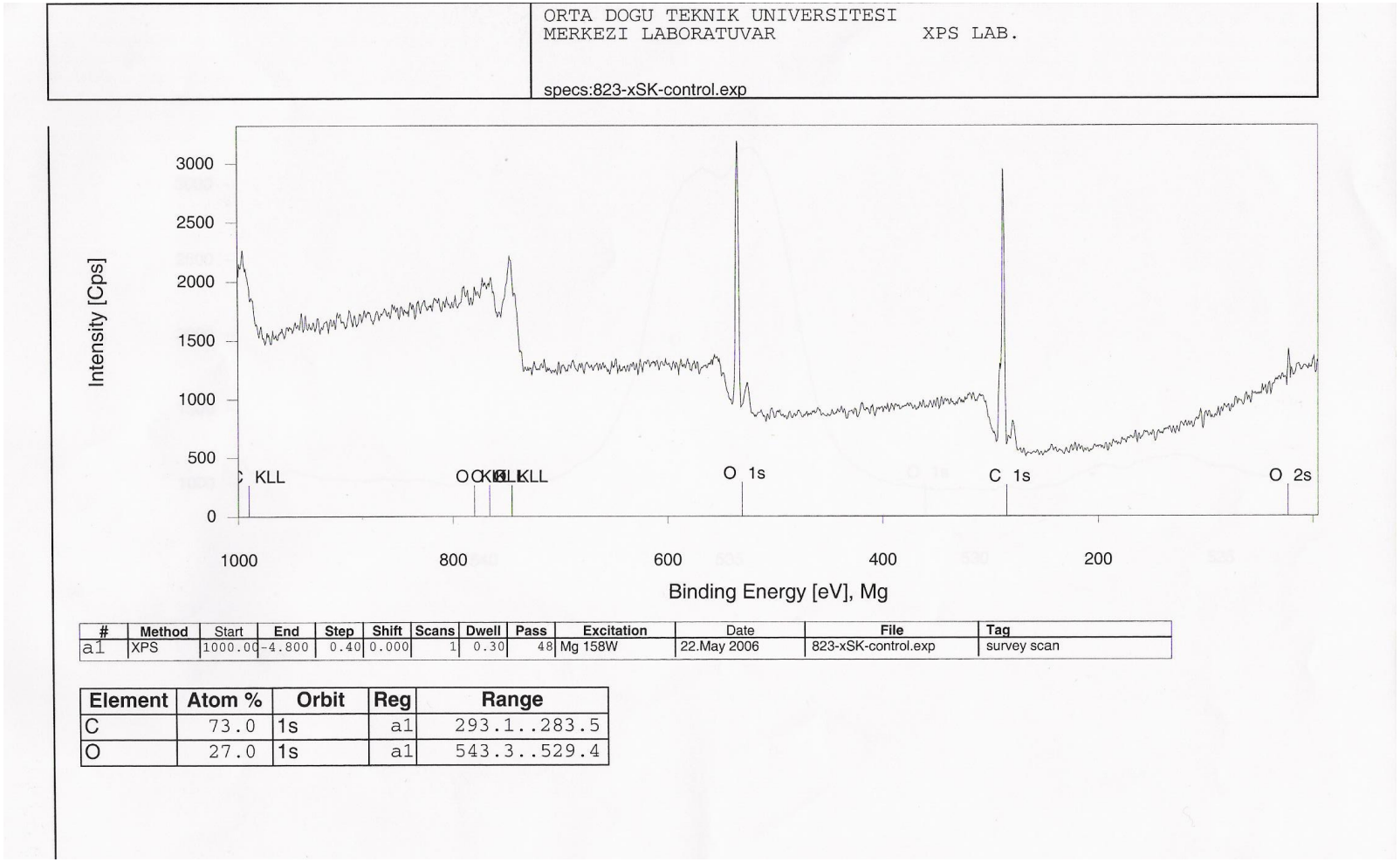

#	Method	Start	End	Step	Shift	Scans	Dwell	Pass	Excitation	Date	File	Tag
a1	XPS	1000.00	-4.800	0.40	0.000	1	0.30	48	Mg 158W	22.May 2006	823-xSK-control.exp	survey scan

Element	Atom %	Orbit	Reg	Range
C	73.0	1s	a1	293.1..283.5
O	27.0	1s	a1	543.3..529.4

Figure 3.15 Esca graph of the untreated PMMA.

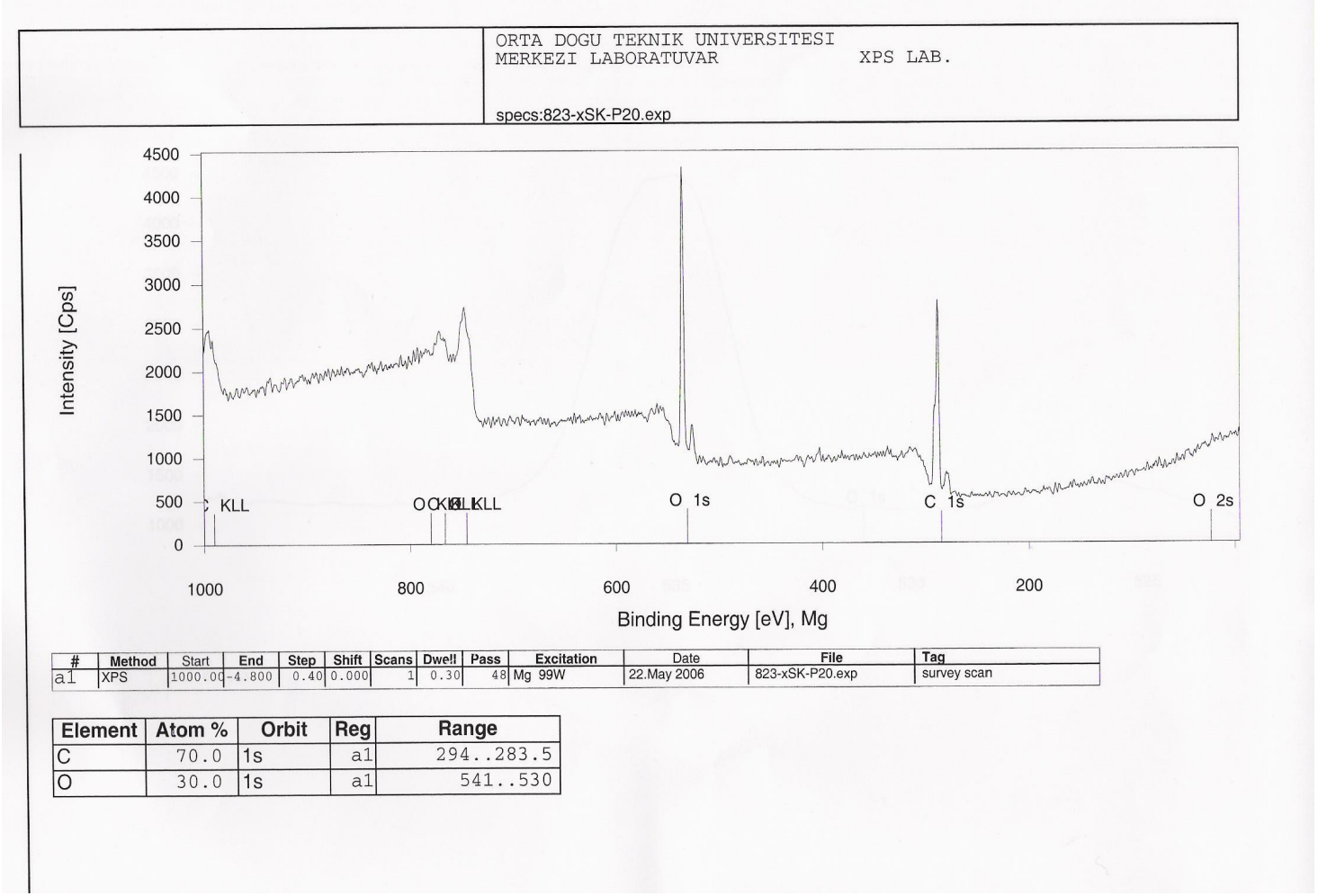

#	Method	Start	End	Step	Shift	Scans	Dwell	Pass	Excitation	Date	File	Tag
a1	XPS	1000.0	-4.800	0.40	0.000	1	0.30	48	Mg 99W	22.May 2006	823-xSK-P20.exp	survey scan

Element	Atom %	Orbit	Reg	Range
C	70.0	1s	a1	294..283.5
O	30.0	1s	a1	541..530

Figure 3.16 Esca graph of 20 W 15 minute plasma applied PMMA.

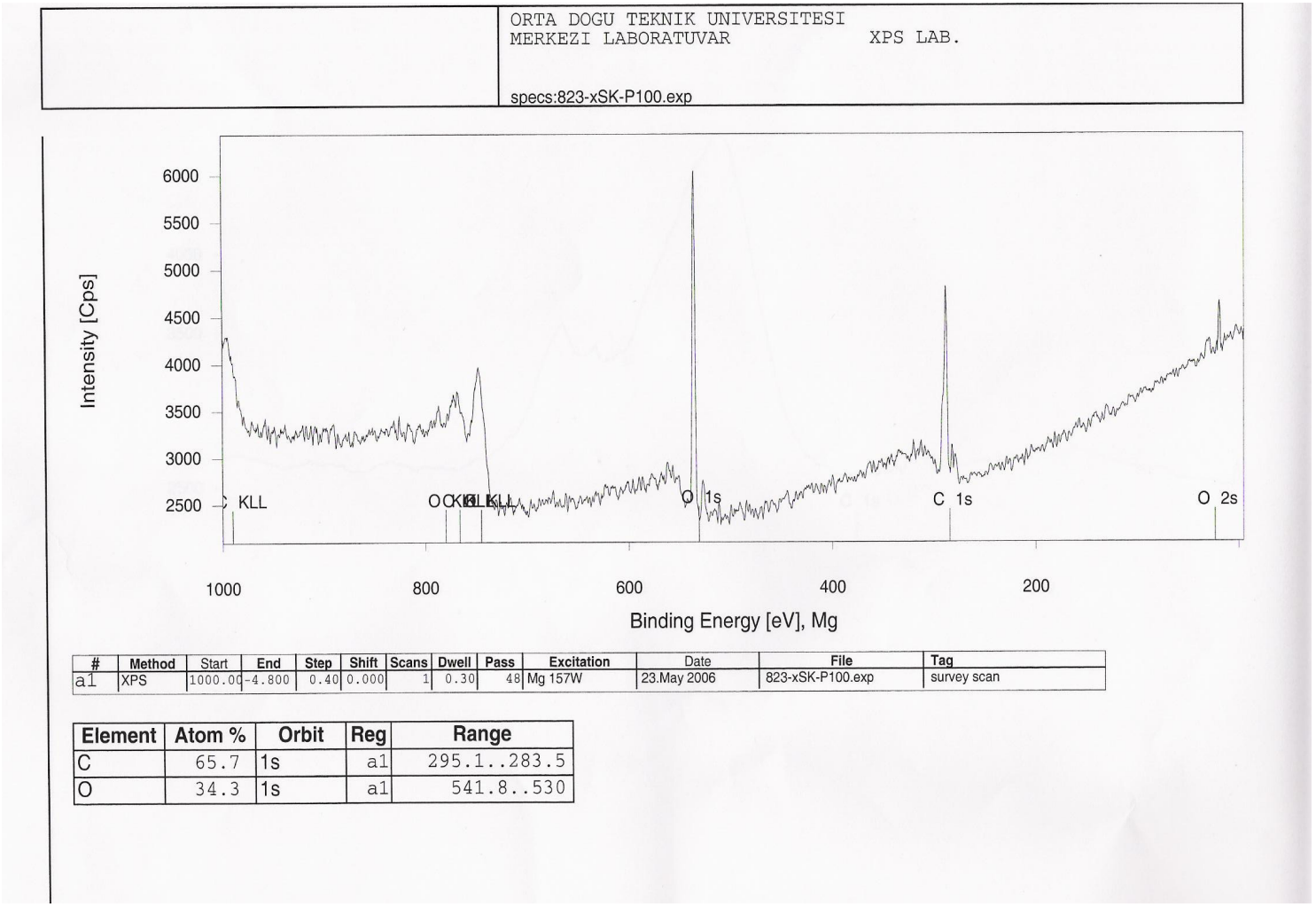

#	Method	Start	End	Step	Shift	Scans	Dwell	Pass	Excitation	Date	File	Tag
a1	XPS	1000.00	-4.800	0.40	0.000	1	0.30	48	Mg 157W	23.May 2006	823-xSK-P100.exp	survey scan

Element	Atom %	Orbit	Reg	Range
C	65.7	1s	a1	295.1..283.5
O	34.3	1s	a1	541.8..530

Figure 3.17 Esca graph of 100 W 15 minute plasma applied PMMA.

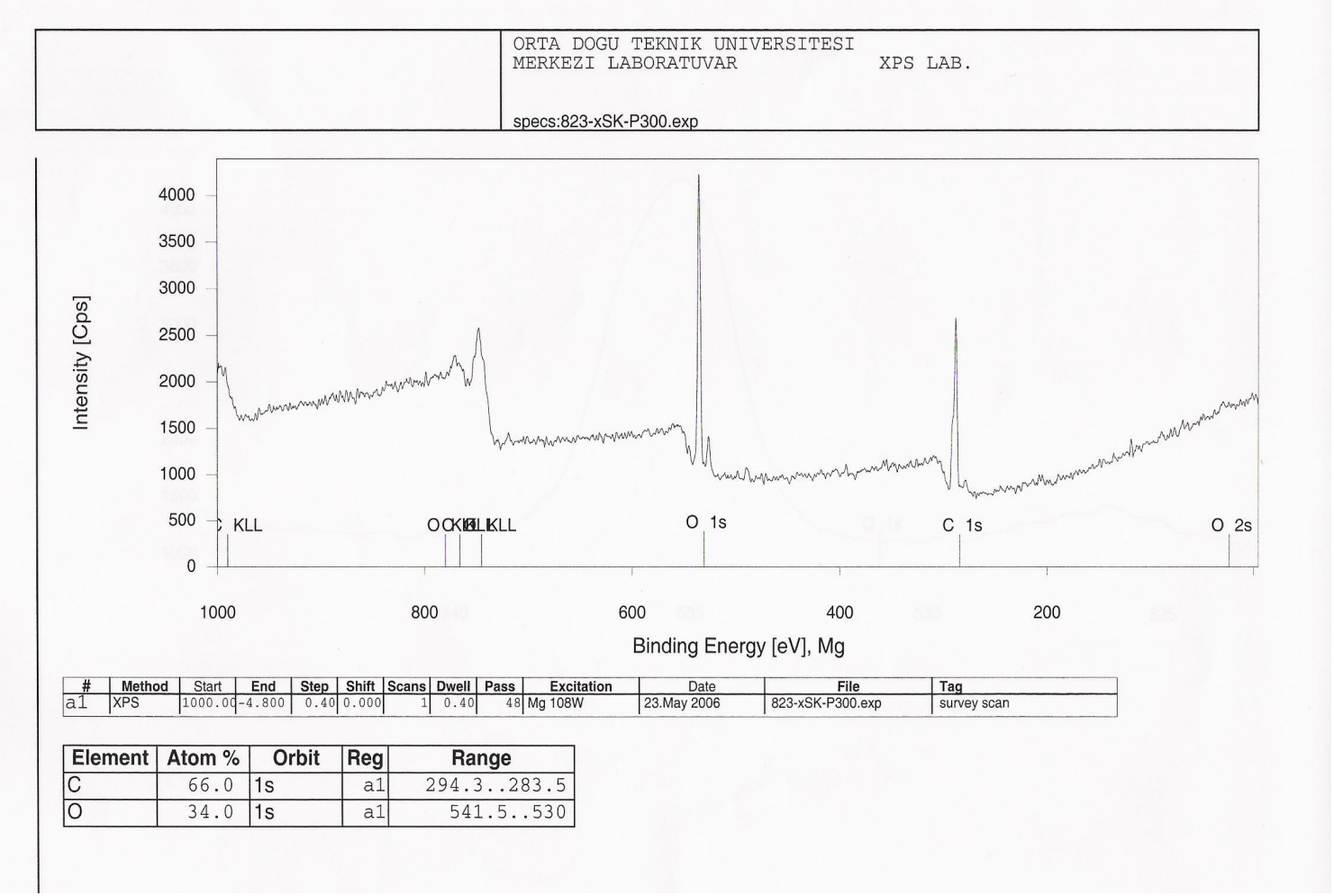

#	Method	Start	End	Step	Shift	Scans	Dwell	Pass	Excitation	Date	File	Tag
a1	XPS	1000.00	-4.800	0.40	0.000	1	0.40	48	Mg 108W	23.May 2006	823-xSK-P300.exp	survey scan

Element	Atom %	Orbit	Reg	Range
C	66.0	1s	a1	294.3..283.5
O	34.0	1s	a1	541.5..530

Figure 3.18 Esca graph of 300 W 15 minute plasma applied PMMA.

One last point to mention is the work of adhesion which was estimated against water and glycerol as given in Table 3.25. Work of adhesion against water is in same trend with plasma application and demonstrated a continuous increase as the power was increased. But work of adhesion for glycerol demonstrated a maximum as it is in cell attachment experiments. Work of adhesion against glycerol first increased from 102.49 mJ/m^2 with an increase in the applied plasma power up to 100 W. Further increase in power caused a decrease. We may say that glycerol, with its hydroxyl groups attached to the carbons, might have showed similarity to the molecules that exist in the structure of a cell membrane.

Table 3.25 Work of adhesion changes with the plasma application of 15 min. with varying powers.

Sample	Work of Adhesion (mJ/m^2)	
	With Water	With Glycerol
Control	104.11	102.49
P-20	129.23	115.77
P-100	131.23	117.36
P-300	136.33	109.39

Work of adhesion is the amount of energy required to separate two materials in touch and it is responsible for adhesion. However the work of adhesion values we calculated here were the ones for solid liquid interfaces. But, if one were to estimate the work of adhesion against cells, they need to know the interfacial tensions between cell and solid γ_{cs} and cell and liquid γ_{cl} which are not impossible but very hard to find values. The work of adhesion would then be calculated from the equation 18.

$$W_{cl} = \gamma_{cl} + \gamma_{sl} - \gamma_{cs} \quad \text{..... 18}$$

CHAPTER 4

CONCLUSIONS

For biomaterials, SFE is a very important parameter, but in general, the methods used for the evaluation of SFE do not give quite similar results with each other [4, 8]. Therefore, in this study to find the SFE, its acidic, basic and dispersive components of PMMA films were examined and their effect on the attachment of the cells which come in contact with the surface of PMMA and plasma modified films were searched.

For any study where SFE of a solid is important, it may be necessary to use various test liquids and apply different approximations to find the components and total SFE values. This would be particularly useful when surface modification of a certain material is to be done. Knowing the appropriate liquid pairs and triplets and most accurate method that works on that material in association to literature would lead to more accurate results for SFE determination before and after the modifications of the surfaces.

Even though the work of Shimizu and Demarquette [8] proposed that better results would be obtained when polar and non polar liquids are used as a pair in the geometric and harmonic mean equations, it has been seen that liquids with similar polarities may also give precise results.

The approximations used by the methods fit quite well for the calculations of total SFE. However, when it comes down to components, the methods deviate from each other. It is evident that the result of SFE is affected by the choices of liquid couples, more, when geometric mean or harmonic mean equations are used.

When all the data for untreated PMMA are considered, the prepared PMMA surface appear to have higher polarity than the literature values.

This may be explained by conformational changes of the molecules which differ by the type of solvent and surface used in the solvent casting method. In this study the solvent was chloroform and the PMMA solution was poured on glass lams and the polar structure of the glass might have resulted in an organization and lead to more polar character.

Plasma application is a good way of surface modification. Surfaces of the prepared PMMA films were modified by plasma technique and mainly the hydrophilicities and the surface free energies of the films changed. Surface free energy and hydrophilicity mainly increased both with the application of rising power by constant treatment time and by increasing the treatment time by constant power.

Among the methods available in the literature, geometric and harmonic mean equations were applied for the determination of the dispersive and polar components of SFE. However, the equations gave quite deviated results after the applications of plasma even though they achieved more precise results for the prepared and untreated PMMA surfaces. Harmonic mean method resulted higher dispersive component and lower polar component compared to geometric mean method.

The results obtained from Geometric and harmonic mean methods were parallel to each other only when total SFE is considered.

The affect of plasma was stronger when plasma is applied for 15 minutes compared to application of 1 minute. Increase in power caused an increase in the polar component of SFE as well as total SFE.

Choice of liquid pair plays an important role when geometric or harmonic mean methods are used. In this study most proportional increase was observed when the pair with highest polarity difference (in this study this couple was water-diethylene glycol) was used.

In most of the literature, only two or three liquid combinations are used in the calculation of SFE [38-44]. Obtaining acidic basic components just by one liquid triplet or obtaining polar and dispersive components

just by one liquid couple might lead on to wrong results. In this study, it was found that many liquids and possible liquid combinations should be tried in the calculation of the components of SFE.

According to Zisman and Saito, SFE increased with plasma power when applied for 15 minutes, however one minute applications were not that effective on SFE.

Aside from increasing SFE, plasma application mainly increased hydrophilicity. Hydrophilicity increased parallel to that of the polar component of SFE.

For plasma modified samples, acid base approach did not give accurate results while Geometric and Harmonic mean methods seem more appropriate due to the possibility that random changes of functionality might have caused random acidic basic component changes.

For all the plasma modified surfaces improved cell attachments were observed. Plasma application increased cell attachment by increasing hydrophilicity up to certain points. Total SFE and its polar component is in trend with cell attachment up to certain point however dispersive component does not seem to have much effect on the cell attachment.

It is expected that there is a critical combination of acidic, basic, dispersive components of SFE which enhance the cell attachment on the surfaces of biomaterials. This study is a first step to enlighten this relation. Although some general trends are observed, still there are much work to do to explain the cell-surface communication.

REFERENCES

[1] Edward C. Combe, Brandon A. Owen, James S. Hodges, "A protocol for determining the surface free energy of dental materials", Dental Materials, 20 (2004) 262–268.

[2] Hacı Ali Gulec, Kemal Sarıoglu, Mehmet Mutlu, "Modification of food contacting surfaces by plasma polymerisation technique. Part I: Determination of hydrophilicity, hydrophobicity and surface free energy by contact angle method", Journal of Food Engineering, 5 (2006) 187-195.

[3] D. Y. Kwok, A. Leung, C. N. C. Lam, A. Li, R. Wu, and A. W. Neumann, "Low-rate dynamic contact angles on poly(methyl methacrylate) and the determination of solid surface tensions", Journal of Colloid and Interface Science 206 (1998) 44 –51.

[4] S. Cantin, M. Bouteau, F. Benhabib, F. Perrot, "Surface free energy evaluation of well-ordered Langmuir–Blodgett surfaces, Comparison of different approaches", Colloids and Surfaces A: Physicochemical and Engineering Aspects, 276 (2005) 107-115.

[5] The Measurement of surface energy of polymer by means of contact angles of liquids on solid surfaces, A short overview of frequently used methods by Finn Knut Hansen, Department of Chemistry, University of Oslo 2006.

[6] K. Vijayanand, Deepak K. Pattanayak, T. R. Rama Mohan and R. Banerjee, "Interpreting Blood-Biomaterial Interactions from Surface Free Energy and Work of Adhesion", Trends in Biomaterials Artificial Organs, 18 (2005) 73-83.

[7] S. Siboni, C. Della Volpe, D. Maniglio, and M. Brugnara, "The solid surface free energy calculation II) The limits of the Zisman and of the equation-of-state approaches", Journal of Colloid and Interface Science, 271 (2004) 454–472.

[8] Renato Norio Shimizu, Nicole Raymonde Demarquaette, "Evaluation of Surface Energy of Solid Polymers Using Different Models", Journal of Applied Polymer Science, 76 (2000) 1831-1845.

[9] Erwin A. Vogler, "Structure and reactivity of water at biomaterial surfaces", Advances in Colloid and Interface Science, 74 (1998) 69-117.

[10] Christian Oehr, "Plasma Surface Modification of Polymers for Biomedical Use", Nuclear Instruments and Methods in Physics Research B, 208 (2003) 40–47.

[11] Plasma Surface Modification in Biomedical Applications, AST Technical Journal, World Wide Web "www.astp.com", 2006.

[12] Xianshuang Yang, Kai Zhao, Guo-Qiang Chen, "Effect of surface treatment on the biocompatibility of microbial polyhydroxyalkanoates", Biomaterials 23 (2002) 1391–1397.

[13] F.-Z Sidouni, N. Nurdin, P Chabrecek, D. Lohmann, J. Vogt, N. Xanthopoulos, H.J. Mathieu, P. Francois, P. Vaudaux, P. Descouts, "Surface properties of a specifically modified high-grade medical polyurethane", Surface Science, 491 (2001) 355-369.

[14] John H. Clint, "Adhesion and components of solid surface energies", Current Opinion in Colloid & Interface Science 6 (2001) 28-33.

[15] D.J. Li, F.Z. Cui, H.Q. Gu, "Cell adhesion of F+ ion implantation of intraocular lens", Nuclear Instruments and Methods in Physics Research B, 152 (1999) 80-88.

[16] Ulrike Schulz, Peter Munzert, Norbert Kaiser, "Surface modification of PMMA by DC glow discharge and microwave plasma treatment for the improvement of coating adhesion", Surface and Coatings Technology, 142-144 (2001) 507-511.

[17] C. Satriano a, S. Carnazza b, S. Guglielmino b, G. Marletta, "Surface free energy and cell attachment onto ion-beam irradiated polymer surfaces", Nuclear Instruments and Methods in Physics Research B, 208 (2003) 287–293.

[18] Erwin A. Vogler, "Thermodynamics of Short-Term Cell Adhesion in Vitro", Biophysics Journal, 53 (1988) 759-769.

[19] L. Hermitte, F. Thomas, R. Bougaran and C. Martelet, "Contribution of comonomers to bulk and surface properties of methacrylate copolymers", Journal of Colloid and Interface Science, 272 (2004) 82-89.

[20] Jie Wang, Chunyan Chen, Sarah M. Buck and Zhan Chen, "Molecular Chemical Structure on Poly(methyl methacrylate) (PMMA) Surface Studied by Sum Frequency Generation (SFG) Vibrational Spectroscopy", J. Phys. Chem. B, 105 (2001) 12118-12125.

[21] H.K. Varmaa, K. Sreenivasana, Y. Yokogawab, A. Hosumi, "In vitro calcium phosphate growth over surface modified PMMA film", Biomaterials, 24 (2003) 297–303.

[22] Nick Silikas, Abdulaziz Al-Kheraif, David C. Watts, "Influence of P/L ratio and peroxide/amine concentrations on shrinkage-strain kinetics during setting of PMMA/MMA biomaterial formulations", Biomaterials, 26 (2005) 197–204.

[23] Seok Bong Kim, Young Jick Kim, Taek Lim Yoon, Su A. Park, In Hee Cho, Eun Jung Kim, In Ae Kim, Jung-Woog Shin, "The characteristics of a hydroxyapatite–chitosan–PMMA bone cement", Biomaterials, 25 (2004) 5715–5723.

[24] Fani Anagnostou, Aurore Debet, Graciela Pavon-Djavid, Zakaryia Goudaby, Gerard Helary, Veronique Migonney, "Osteoblast functions on functionalized PMMA-based polymers exhibiting Staphylococcus aureus adhesion inhibition", Biomaterials, 27 (2006) 3912–3919.

[25] Sang-Hoon Rhee, Mi-Hye Hwang, Hyun-Jung Si, Je-Yong Cho, "Biological activities of osteoblasts on poly(methyl methacrylate)/silica hybrid containing calcium salt", Biomaterials, 24 (2003) 901–906.

[26] Daniele Tognetto, Giuseppe Ravalico, "Inflammatory cell adhesion and surface defects on heparin-surface-modified poly(methyl methacrylate) intraocular lenses in diabetic patients", Cataract Refract Surgery, 27 (2001) 239-244.

[27] Shyam Patel, Rahul G. Thakar, Josh Wong, Stephen D. McLeod, Song Li, "Control of cell adhesion on poly(methyl methacrylate)", Biomaterials, 27 (2006) 2890–2897.

[28] Catharina Latz, Graciela Pavon-Djavid, Gerard Helary, Margaret DM Evans and Veronique Migonney, "Alternative Intracellular Signaling Mechanism Involved in the Inhibitory Biological Response of Functionalized PMMA-Based Polymers", Biomacromolecules, 4 (2003) 766-771.

[29] C. Della Volpe, D. Maniglio, M. Brugnara, S. Siboni, and M. Morra, "The solid surface free energy calculation I) In defense of the multicomponent approach", Journal of Colloid and Interface Science, 271 (2004) 434–453.

[30] Emil Chibowski, Rafael Perea-Carpio, "Problems of contact angle and solid surface free energy determination", Advances in Colloid and Interface Science, 98 (2002) 245-264.

[31] Torun Köse G., Kenar H., Hasırcı N., Hasırcı V., "Macroporous poly(3-hydroxybutyrate-co-3-hydroxyvalerate) matrices for bone tissue engineering", Biomaterials, 24 (2003) 1949-1958.

[32] Edward C. Combea, Brandon A. Owena, James S. Hodgesb, "A protocol for determining the surface free energy of dental materials", Dental Materials, 20 (2004) 262–268.

[33] Halina Kaczmarek, Hanna Chaberska, "The influence of UV-irradiation and support type on surface properties of poly(methyl methacrylate) thin films ", Applied Surface Science, Article in Press (2005).

[34] K.S. Birdi, Handbook of surface and colloid chemistry, CRC Press, Second edition, pp.103 (2003).

[35] Jinan Chai, Fuzhi Lu, Baoming Li, and Daniel Y. Kwok, "Wettability Interpretation of Oxygen Plasma Modified Poly(methyl methacrylate)", Langmuir, 20 (2004) 10919 -10927.

[36] A. Said, A. Mavon , S. Makki , Ph. Humbert , J. Millet, "Wettability of psoralen powders: influence of bile salts on their contact angles and surface free energy components", Colloids and Surfaces B: Biointerfaces, 8 (1997) 227 - 237.

[37] Ulrike Schulz, Peter Munzert, Norbert Kaiser, "Surface modification of PMMA by DC glow discharge and microwave plasma treatment for the improvement of coating adhesion", Surface and Coatings Technology 142-144 (2001) 507-511.

[38] Y.-S. Lin, C.-H. Chang, T.-J. Huang, "A study of the low temperature plasma polymerization on enhancing interface of painted cold rolled steel in salt bath", Surface & Coatings Technology, 200 (2006) 3355 - 3365.

[39] Oh-June Kwon, Sung-Woon Myung, Chang-Soo Lee, Ho-Suk Choi, "Comparison of the surface characteristics of polypropylene films treated by Ar and mixed gas (Ar/O2) atmospheric pressure plasma", Journal of Colloid and Interface Science, 295 (2006) 409 - 416.

[40] Zhong Zhi You, Jiang Ya Dong, "Effect of oxygen plasma treatment on the surface properties of tin-doped indium oxide substrates for polymer LEDs", Journal of Colloid and Interface Science, Article in press.

[41] H.S. Choi,, V.V. Rybkin, V.A. Titov, T.G. Shikova, T.A. Ageeva, "Comparative actions of a low pressure oxygen plasma and an atmospheric pressure glow discharge on the surface modification of polypropylene", Surface & Coatings Technology, 200 (2006) 4479 - 4488.

[42] Soo-Jin Park and Jeong-Soon Kim, "Influence of Plasma Treatment on Microstructures and Acid–Base Surface Energetics of Nanostructured Carbon Blacks: N2 Plasma Environment", Journal of Colloid and Interface Science, 244 (2001) 336 - 41.

[43] Mariana D. Duca, Carmina L. Plosceanu & Tatiana Pop, "Surface modifications of polyvinylidene fluoride (PVDF) under rf Ar plasma" Polymer Degradation and Stability, 61 (1998) 65 - 72.

[44] Oh-June Kwon, Shen Tang, Sung-Woon Myung, Na Lu, Ho-Suk Choi, "Surface characteristics of polypropylene film treated by an atmospheric pressure plasma", Surface & Coatings Technology 192 (2005) 1–10.